J. Dairy Sci. 107:6288–6307
https://doi.org/10.3168/jds.2024-24346

Bile acid profiles and mRNA abundance of bile acid-related genes in adipose tissue of dairy cows with high versus normal body condition

Lena Dicks,[1] Katharina Schuh-von Graevenitz,[2] Cornelia Prehn,[3] Hassan Sadri,[4] Eduard Murani,[5] Morteza Hosseini Ghaffari,[1] and Susanne Häussler[1]*

[1]Institute of Animal Science, Physiology Unit, University of Bonn, 53115 Bonn, Germany
[2]Department of Life Sciences and Engineering, Animal Nutrition and Hygiene Unit, University of Applied Sciences Bingen, 55411 Bingen am Rhein, Germany
[3]Helmholtz Zentrum München, German Research Center for Environmental Health, Metabolomics and Proteomics Core, 85764 Neuherberg, Germany
[4]Department of Clinical Science, Faculty of Veterinary Medicine, University of Tabriz, 516616471 Tabriz, Iran
[5]Research Institute for Farm Animal Biology (FBN), Institute for Genome Biology, Wilhelm-Stahl-Allee 2, 18196 Dummerstorf, Germany

ABSTRACT

Besides their lipid-digestive role, bile acids (BA) influence overall energy homeostasis, such as glucose and lipid metabolism. We hypothesized that BA along with their receptors, regulatory enzymes, and transporters are present in subcutaneous adipose tissue (scAT). In addition, we hypothesized that their mRNA abundance varies with the body condition of dairy cows around calving. Therefore, we analyzed BA in serum and scAT as well as the mRNA abundance of BA-related enzymes, transporters, and receptors in scAT during the transition period in cows with different body conditions around calving. In a previously established animal model, 38 German Holstein cows were divided into either a high (HBCS; n = 19) or normal BCS (NBCS; n = 19) group based on their BCS and back-fat thickness (BFT). Cows were fed different diets to achieve the targeted differences in BCS and BFT (NBCS: BCS <3.5, BFT <1.2 cm; HBCS: BCS >3.75, BFT >1.4 cm) until dry-off at 7 wk antepartum. During the dry period and subsequent lactation, both groups were fed the same diets according to their energy demands. Using a targeted metabolomics approach via liquid chromatography-electrospray ionization-MS /MS, BA were analyzed in serum and scAT at wk −7, 1, 3, and 12 relative to parturition. In serum, 15 BA were observed: cholic acid (CA), chenodeoxycholic acid (CDCA), glycocholic acid (GCA), taurocholic acid (TCA), glycochenodeoxycholic acid (GCDCA), taurochenodeoxycholic acid, deoxycholic acid (DCA), lithocholic acid, glycodeoxycholic acid (GDCA), glycolithocholic acid, taurodeoxycholic acid, taurolithocholic acid, β-muricholic acid, tauromuricholic acid (sum of α and β), and glycoursodeoxycholic acid, whereas in scAT 7 BA were detected: CA, GCA, TCA, GCDCA, taurochenodeoxycholic acid, GDCA, and taurodeoxycholic acid. In serum and scAT samples, the primary BA CA and its conjugate GCA were predominantly detected. Increasing serum concentrations of CA, CDCA, TCA, GCA, GCDCA, DCA, and β-muricholic acid with the onset of lactation might be related to the increasing DMI after parturition. Furthermore, serum concentrations of CA, CDCA, GCA, DCA, GCDCA, TCA, lithocholic acid, and GDCA were lower in HBCS cows compared with NBCS cows, concomitant with increased lipolysis in HBCS cows. The correlation between CA in serum and scAT may point to the transport of CA across cell membranes. Overall, the findings of the present study suggest a potential role of BA in lipid metabolism depending on the body condition of periparturient dairy cows.

Key words: adipose tissue, bile acids, body condition, periparturient period

INTRODUCTION

Bile acids (**BA**) are formed in the liver from cholesterol and are synthesized by various enzymatic processes within the classical/neutral or alternative/acidic synthetic pathways (Russell, 2003; Ma and Patti, 2014; Shapiro et al., 2018). Although BA classically facilitate the digestion and absorption of nutrients such as lipids and lipophilic vitamins from the intestine, they also act as signaling molecules and can influence glucose and lipid metabolism (Ferrebee and Dawson, 2015; Shapiro et al., 2018).

The primary BA, cholic acid (**CA**) and chenodeoxycholic acid (**CDCA**), are synthesized in the liver and conjugated by the amino acids glycine or taurine to form the conjugated primary BA (Armstrong and Carey, 1982). After feed intake, the enterohormone cholecysto-

Received October 25, 2023.
Accepted February 14, 2024.
*Corresponding author: susanne.haeussler@uni-bonn.de

The list of standard abbreviations for JDS is available at adsa.org/jds-abbreviations-24. Nonstandard abbreviations are available in the Notes.

kinin stimulates gallbladder contraction, and the BA are released into the intestine where they are deconjugated and 7α-dehydroxylated by intestinal bacteria. Finally, the resulting secondary BA (Di Ciaula et al., 2017) can be conjugated in the intestine by either glycine or taurine (Chiang, 2004). The BA biosynthetic pathway is shown in Figure 1.

In humans, the majority of BA (90%–95% in total) return to the liver at the terminal ilium via the portal vein; however, BA that are not reabsorbed are excreted via feces (Yang et al., 2003; Chiang, 2004; Chen et al., 2019a,b). Moreover, a small portion of BA enters the systemic circulation (Hofmann, 2009). In addition to enterohepatic circulation, BA have also been detected in tissues such as the kidney and heart in rats (Swann et al., 2011), bovine follicular fluid (Blaschka et al., 2020), and human adipose tissue (**AT**; Jäntti et al., 2014). Furthermore, a variety of different BA transporters have been

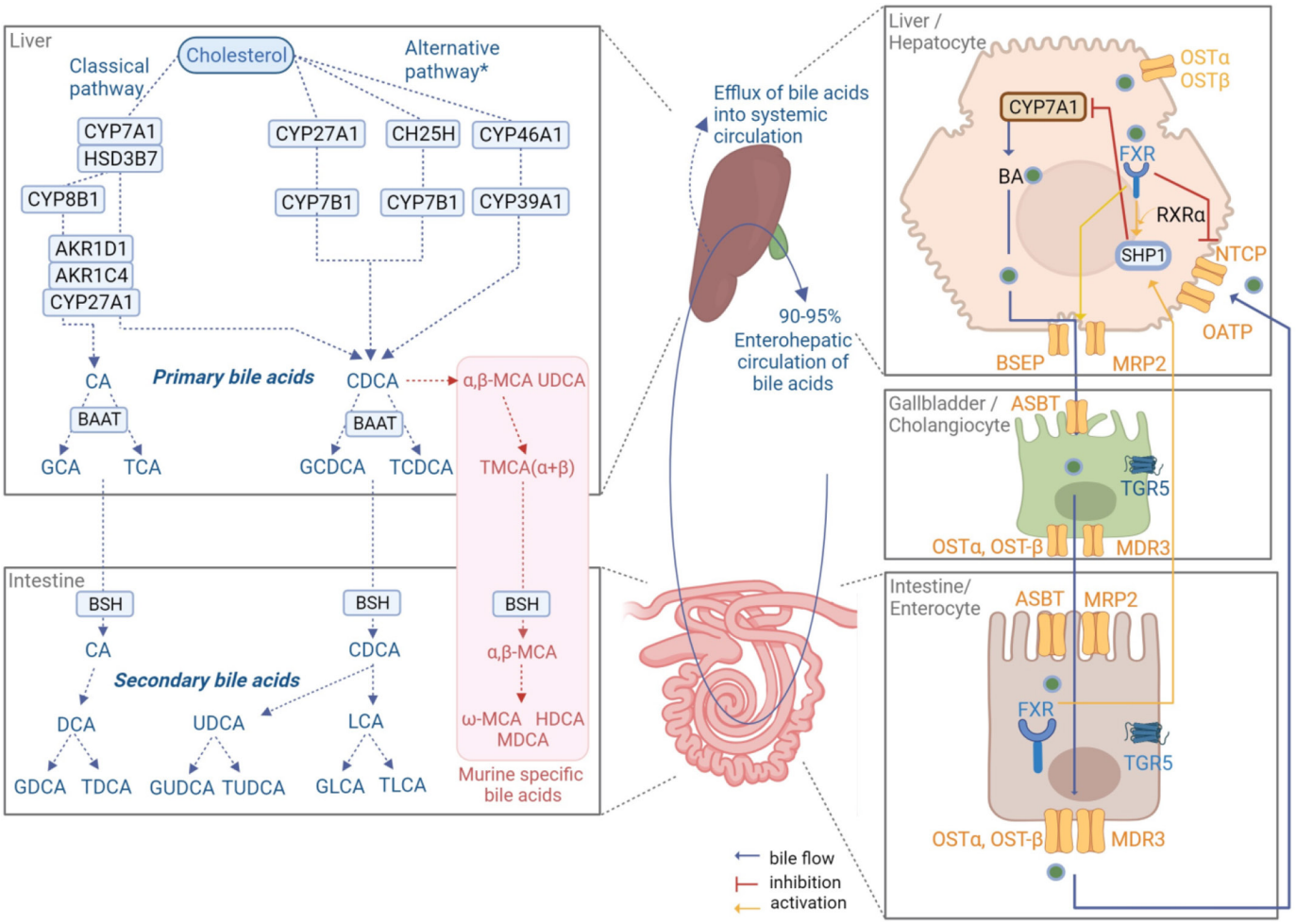

Figure 1. Bile acid synthesis pathway in liver and intestine. *Bile acid-related enzymes are ubiquitously expressed and not limited to the hepatic alternative pathway. Involved enzymes include CYP7A1: cholesterol 7alpha-hydroxylase; HSD3B7: 3 beta-hydroxysteroid dehydrogenase type 7; CYP8B1: sterol 12-alpha-hydroxylase; AKR1D1: aldo-keto reductase family 1 member D1; AKR1C4: aldo-keto reductase family 1 member C4; CYP27A1: sterol 27-hydroxylase; CYP7B1: oxysterol 7-alpha-hydroxylase; CH25H: cholesterol 25-hydroxylase; CYP46A1: cholesterol 24-hydroxylase; CYP39A1: cytochrome P450 family 39 subfamily A member 1; BAAT: bile acid coenzyme A: amino acid N-acyltransferase; BSH: bile salt hydrolase transporters: NTCP, SLC10A1: Na^+-taurocholate cotransporting polypeptide; SLC10A2, ASBT: apical sodium-dependent bile acid transporter; OSTα, SLC51A1: solute carrier family 51 subunit α; OSTβ, SLC51B: solute carrier family 51 subunit β; MRP2, ABCC2: multidrug resistance-associated protein; BSEP, ABCB11: bile salt export pump; MDR3, ABCB4: multiple drug resistance 3; OATP: solute carrier organic anion transporter. Receptors include FXR, NR1H4: farnesoid X receptor; TGR5, GPBAR1: Takeda G protein-coupled receptor 5; RXRα, NR2B1: retinoid X receptor alpha; SHP: small heterodimer partner. Bile acids include cholic acid (CA), chenodeoxycholic acid (CDCA), taurocholic acid (TCA), glycocholic acid (GCA), taurochenodeoxycholic acid (TCDCA), glycochenodeoxycholic acid (GCDCA), deoxycholic acid (DCA), lithocholic acid (LCA), ursodeoxycholic acid (UDCA) taurodeoxycholic acid (TDCA), glycodeoxycholic acid (GDCA), taurolithocholic acid (TLCA), glycolithocholic acid (GLCA), glycoursodeoxycholic acid (GUDCA), tauroursodeoxycholic acid (TUDCA), α-muricholic acid (αMCA), β-muricholic acid (βMCA), tauromuricholic acid (sum of α and β; α, β-TMCA), ω-muricholic acid (ωMCA), hyodeoxycholic acid (HDCA), murideoxycholic acid (MDCA). The figure was created using BioRender (SL25XUBGY1).

described to control BA flux, either by absorption and enterohepatic circulation or by excretion and elimination from the body (Dawson et al., 2009).

In mice and humans, BA activate both nuclear and membrane receptors (Ticho et al., 2019). The farnesoid X receptor (**FXR**) is considered to be a metabolic feedback sensor for the formation of BA by inhibiting the transcription of BA-forming enzymes (Chiang, 2009). Moreover, the Takeda G protein-coupled receptor 5 (**TGR5**) is expressed in many murine tissues, such as the placenta, gallbladder, liver, intestine, and brown AT (Maruyama et al., 2002; Maruyama et al., 2006). Via TGR5, BA stimulate energy expenditure in brown AT and skeletal muscle of mice (Watanabe et al., 2006). Furthermore, several membrane and nuclear receptors such as the nuclear receptors vitamin D receptor (**VDR**), pregnane X receptor (NR1I2), and constitutive androstane receptor (NR1I3), G protein-coupled sphingosine-1-phosphates receptor 2 (S1PR2), can be activated by BA and indirectly affect BA homeostasis (Kliewer et al., 1998; Timsit and Negishi, 2007; Wan and Sheng, 2018; Studer et al., 2012).

In the periparturient period, lipid mobilization, mainly from AT, can affect the metabolism of dairy cows (Drackley et al., 2005). Cows with higher precalving body condition mobilize more body reserves after parturition and are therefore more prone to metabolic disorders compared with thinner cows (Bernabucci et al., 2005). Increased lipid mobilization from AT, which is associated with an increase in free fatty acids in the blood, may increase the risk of metabolic diseases such as ketosis and fatty liver (Adewuyi et al., 2005). Dairy cows suffering from the fatty liver syndrome had increased plasma concentrations of bile components, that is, bilirubin (West, 1990) and BA (Rehage et al., 1999), indicating a decrease in bile flow. In dairy cows, plasma BA profiles were affected after excessive lipolysis around calving (Gu et al., 2023); however, BA profiles in bovine scAT have not yet been investigated. In the present study, we aimed to investigate BA in serum and scAT by a metabolomics approach, as well as the mRNA abundance of BA-related enzymes, receptors, and transporters by quantitative reverse-transcription real-time PCR (**RT-qPCR**) in scAT from dairy cows with different body conditions. We hypothesized that (1) cows with different precalving body conditions and thus different levels of lactation-induced lipolysis would differ in their BA profiles and (2) BA, as well as the mRNA abundances of BA receptors, transporters, and regulatory enzymes, are present in subcutaneous AT (scAT) of dairy cows. By investigating variables involved in BA metabolism within bovine scAT, we aimed to further elucidate lipid metabolism in the periparturient period of dairy cows.

MATERIALS AND METHODS

Basic Trial

The animal experiment was performed at the Educational and Research Centre for Animal Husbandry, Hofgut Neumuehle, Muenchweiler a.d. Alsenz, Germany. The trial was conducted following European regulations for the protection of experimental animals and was approved by the local authority for animal welfare affairs (Landesuntersuchungsamt Rheinland-Pfalz, Koblenz, Germany [G 14–20–071]). The experiment was described previously in detail (Schuh et al., 2019). In brief, the experimental period started 15 wk before calving and lasted until 14 wk after calving. In total, 38 multiparous German Holstein cows were preselected based on their BCS and back-fat thickness (**BFT**) of the previous lactation and divided into 2 groups: high BCS (**HBCS**; n = 19) and normal BCS (**NBCS**; n = 19). They received different feeding regimens from 15 wk antepartum (**a.p.**) to 7 wk a.p. (HBCS: 7.2 NE_L MJ/kg of DM; NBCS: 6.8 NE_L MJ/kg of DM) to reach the targeted BCS and BFT at dry-off (HBCS: BCS >3.75 and BFT >1.4 cm; NBCS: BCS <3.5 and BFT <1.2 cm). During the dry period and subsequent lactation, both groups received identical diets. Performance data (BCS, BFT, energy balance, and DMI) were reported earlier (Schuh et al., 2019) and are presented herein as Supplemental Figures S1, S2, S3, and S4, respectively (see Notes).

Sampling and BA Analyses

Blood and tissue samples were collected at wk 7 a.p., as well as wk 1, 3, and 12 postpartum (**p.p.**). Blood samples were collected from the coccygeal vein after morning milking and before the new presentation of fresh feed. The scAT taken from the tail head region were rinsed with 0.9% NaCl solution and immediately frozen in liquid nitrogen. Samples were stored at −80°C until analysis.

Bile acids in serum and scAT have been quantified using the AbsoluteIDQ Bile Acids kit (Biocrates Life Sciences AG, Innsbruck, Austria). This standardized assay includes sample preparation and liquid chromatography-electrospray ionization-MS/MS (**LC-ESI-MS/MS**) measurements. The assay allows simultaneous quantification of 20 BA, including CA, CDCA, deoxycholic acid (**DCA**), glycocholic acid (**GCA**), glycochenodeoxycholic acid (**GCDCA**), glycodeoxycholic acid (**GDCA**), glycolithocholic acid (**GLCA**), glycoursodeoxycholic acid (**GUDCA**), hyodeoxycholic acid, lithocholic acid (**LCA**), α-muricholic acid, β-muricholic acid, ω-muricholic acid, taurocholic acid (**TCA**), taurochenodeoxycholic acid (**TCDCA**), taurodeoxycholic acid (**TDCA**), taurolitho-

cholic acid (**TLCA**), tauromuricholic acid (sum of α and β), tauroursodeoxycholic acid, and ursodeoxycholic acid. Identification and quantification of the compounds were based on scheduled multiple reaction measurements. The method of the BA kit method has been proven to be in conformance with the EMEA *Guideline on Bioanalytical Method Validation* (EMEA, 2011), which implies proof of reproducibility within a given error range. The complete assay procedures of the BA kit for the analysis of plasma or serum and the results of an interlaboratory ring-trial have been described in detail previously (Pham et al., 2016; McCreight et al., 2018).

Serum samples were applied directly to the assay, whereas scAT samples were applied as homogenate supernatant. The homogenization and extraction protocol were developed specifically for this application. Samples from scAT were prepared as follows: frozen bovine AT samples were weighed into homogenization tubes with ceramic beads (1.4 mm). To ensure comparable extraction efficiency and to provide stable pH values, 12 µL of a cooled (4°C) mixture of ethanol/phosphate buffer (70/30 vol/vol) was added per 1 mg frozen AT. These tissue/buffer samples were homogenized using a Precellys24 homogenizer (PEQLAB Biotechnology GmbH, Germany) 4 times for 20 s at 5,500 × *g* and 10°C to 15°C, with 30-s pause intervals to ensure constant temperature. After sample centrifugation at 10,000 × *g* for 5 min at 15°C, supernatants were used for metabolite quantification.

Internal standards were included in the BA kit and were added after homogenization of scAT. To prepare the assay, 10 µL of the internal standard solution in methanol was pipetted onto the filter inserts of the 96-well sandwich plate. After drying the filters for 5 min at room temperature in a stream of nitrogen, 10 µL of blank, calibration standards, quality control samples, or plasma samples, or 40 µL of the freshly prepared tissue homogenate were pipetted into the respective wells and the filters were dried again for 5 min. The tissue homogenates (40 µL) were applied in 2 steps of 20 µL each, with a separate drying step in between to avoid sample leakage from the filter insert. For extraction of metabolites and internal standards, 100 µL of methanol was added and the plate was shaken at 650 × *g* for 20 min. The metabolite extracts were eluted into the lower deep-well plate by a centrifugation step (5 min at 500 × *g* at room temperature). The upper filter plate was removed, the extracts were diluted with 60 µL of ultrapure water, and the plate was shaken at 450 × *g* for 5 min and placed in the cooled autosampler (10°C) for LC-ESI-MS/MS measurements.

The LC separation was performed using 10 m*M* ammonium acetate in a mixture of ultrapure water/formic acid vol/vol 99.85/0.15 as mobile phase A and 10 m*M* ammonium acetate in a mixture of methanol/acetonitrile/ultrapure water/formic acid vol/vol/vol/vol 30/65/4.85/0.15 as mobile phase B. The BA were separated on the ultra-HPLC column for the BA kit (Product No. 91220052120868) combined with the precolumn SecurityGuard ULTRA Cartridge C18/XB-C18 (for 2.1 mm ID column, Phenomenex Cat. No. AJ0–8782). All solvents used for sample preparation and measurement were of HPLC grade.

Samples were processed using a Hamilton Microlab STAR robot (Hamilton Bonaduz AG, Bonaduz, Switzerland), an Ultravap nitrogen evaporator (Porvair Sciences, Leatherhead, UK), and standard laboratory equipment. Mass spectrometric analyzes were performed using an API 4000 triple quadrupole system (SCIEX Deutschland GmbH, Darmstadt, Germany) equipped with a 1260 series HPLC (Agilent Technologies Deutschland GmbH, Böblingen, Germany) and an HTC-xc PAL autosampler (CTC Analytics, Zwingen, Switzerland) controlled by Analyst 1.6.2 software. Data evaluation for quantification of metabolite concentrations and quality assessment were performed using MultiQuant 3.0.1 (Sciex) software and the MetIDQ software package, which is an integral part of the BA kit. Metabolite concentrations were calculated using internal standards and reported in µmol.

Primer Design and Quantitative Real-Time PCR

Bovine-specific primer pairs were designed using the National Center for Biotechnology Information primer blast. In addition, 8 reference genes, low-density lipoprotein receptor related protein 10 (*LRP10*), glyceraldehyde-3-phosphate dehydrogenase (*GAPDH*), RNA polymerase II (*POLR2A*), eukaryotic translation initiation factor 3, subunit K (*EIF3K*), marvel domain containing 1 (*MARVELD1*), hippocalcin-like 1 (*HPCAL1*), emerin (*EMD*), and tyrosine 3-monooxygenase/tryptophan 5-monooxygenase activation protein zeta (*YWHAZ*), previously shown to be stable in bovine AT (Saremi et al., 2012), were measured. The primer pairs used in this study are presented in Table 1. Specific primers were selected based on an optimal melting temperature of 59°C. Using a Bio-Rad CFX cycler each primer pair was tested by RT-qPCR in pooled cDNA samples from scAT. Primers were tested according to the following RT-qPCR protocol: 3 min at 90°C initial denaturation and 40 cycles of amplification (95°C for 30 s, 59°C for 60 s, and 72°C for 60 s).

RT-qPCR Measurements

The mRNA abundance of 26 target genes and 8 reference genes in scAT from 38 cows at 4 time points was measured by RT-qPCR using the Biomark HD 96.96 system (Fluidigm Co., San Francisco, CA), as described in detail previously (Alaedin et al., 2021). In brief, samples

Table 1. Characteristics of primers and quantitative reverse-transcription real-time PCR conditions

Gene[1]	Target	Sequence[2] 5′-3′	Primer	Accession number	Base pairs
Enzyme					
CYP7A1		F	CTACCCAGACCCGTTGACTT	NM_001205677	270
		R	GGTAAAATGCCCAAGCCTGC		
HSD3B7		F	CCCAGGAGACACAGAAGACC	NM_001034696.1	74
		R	CGGCCATACCTGGCTGC		
CYP8B1		F	GGGAAGGCTTGGAGGAGC	NM_001076139.2	142
		R	GGAGGTGATGAGGAGCCAGA		
AKR1D1		F	ACTCGGAACCTAAATCGACTCC	NM_001192358.1	103
		R	TTCTGGTAGAGGTAGGCCCC		
CYP27A1		F	GGCTGGAGTAGACACGACAT	NM_001083413.2	201
		R	GGGACCACAGGATAGAGACG		
CYP7B1		F	ACAATTGGACAGCCTGGTCT	XM_025001826.1	220
		R	ACTGGAAAATAGCAGCCCATCT		
CH25H		F	ACGCTTGAGGTGGACTTGAG	NM_001075243.1	375
		R	AATCTGAGTCACTGCCCAGC		
CYP46A1		F	TTTCCTTCTAGGGCACCTCC	NM_001076810.1	96
		R	CCGTACTTCTTAGCCCAATCC		
BAAT		F	ACCTGCCTTTCAGAGTGGAG	XM_015472664.1	90
		R	CTGGCCCAAGGACCTTAGTAT		
Transporter					
SLC10A1	*NTCP*	F	GCTATGTCACCAAGGGAGGG	NM_001046339.1	272
		R	GGGGAAGGTCACATTGAGGA		
SLC10A2	*ASBT*	F	TTTCCTTCCAGCGTCAGCAT	XM_019971692.1	566
		R	TATACCACGTACACTGCCAGG		
SLC51A1	*OSTα*	F	CCCAGCTTTTGAGAGCCATC	NM_001025333.2	676
		R	GGTGAACAAGCAATCTGCCC		
SLC51B	*OSTβ*	F	AGCAGACCAGACGAGTCCT	NM_001077867.2	261
		R	TTCCAAGGAGTTGCGTCCTC		
ABCC2	*MRP2*	F	GATGAGGCCACAGTCAATGAG	XM_024985942.1	81
		R	CACGTCCTCTGGGATTTCCT		
ABCB1	*MDR1*	F	GCGGCTCTTCAAGACTCAGTG	XM_024991021.1	137
		R	AGATCCATCGCGACCTCGG		
ABCB11	*BSEP*	F	GCACTGAGTAAGGTTCAGCA	NM_001192703.3	241
		R	TCTCAAGTAAGGCATCTTCGG		
ABCB4	*MDR3*	F	TGGGGCCGGACACTCT	XM_024991318.1	395
		R	TTAGCTTGGCTGCTGCTGA		
Receptor					
NR1H4	*FXR*	F	AAGCCCGCTAAAGGTGTACT	NM_001034708.2	298
		R	TGATTCTCCCTGCTGATGCT		
GPBAR1	*TGR5*	F	GACCTCAACGGTCAGGACAC	NM_175049.3	126
		R	GGCATGCATGACTGTAGGTG		
NR1I2	*PXR*	F	GCGGCATGAGAAAAGAGATGAT	NM_001103226.1	998
		R	AGCCAGTCAGCCATTTGTG		
S1PR2	*S1PR2*	F	GATCGGCCTAGCCAGCATCA	NM_001081541.1	650
		R	AAGATGGTCACCACGCAGAG		
VDR	*VDR*	F	CACCCGCAGGACCAGAGTC	NM_001167932.2	701
		R	GAGAAGCTGGTTGGCTCCAT		
CHRM2	*CHRM2*	F	ACCTCCAGACCGTCAACAAT	NM_001080733.1	139
		R	CAAAGGTCACACACCACAGG		
NR2B1	*RXRα*	F	CCATTTTCGACAGGGTGCTG	NM_001304343.1	171
		R	CCAGGGACGCATAGACCTTC		
SHP1	*SHP1*	F	TCCTCTTCAACCCTGACGTG	XM_002685759.5	173
		R	GCTGGGTGGAATGGACTTGA		
NR1I3	*CAR*	F	GAACAACGGAGGCTACACAC	NM_001079768.2	197
		R	TGTTGACTGTTCGCCTGAAG		
Reference gene					
YWHAZ		F	CCACCTACTCCGGACACAG	NM_174814.2	464
		R	GACTGGTCCACAATCCCTTTC		
EIF3K		F	CCAGGCCCACCAAGAAGAA	NM_001034489	125
		R	TTATACCTTCCAGGAGGTCCATGT		
HPCAL1		F	GCCGGCTTCCTTTTGTCTTT	NM_001098964	216
		R	CTAGACCATGCCCTGCTCC		
POLR2A		F	CTATCGCAGAACCCACTCACC	NM_001206313.2	91
		R	CACAGCGGGAAGGATGTCTG		
GAPDH		F	GAAGGTCGGAGTGAACGGATTC	NM_001034034.2	153

Continued

Table 1 (Continued). Characteristics of primers and quantitative reverse-transcription real-time PCR conditions

Gene[1]	Target	Sequence[2] 5′-3′	Primer	Accession number	Base pairs
		R	TTGCCGTGGGTGGAATCATA		
MARVELD1		F	TCGGTGCTTTGATGTCTTGC	NM_001101262.1	71
		R	CAATCCACGGGCACTTCCTA		
LRP10		F	TTTTCCCGAATCCTGCCTGT	NM_001100371.1	73
		R	ACAGGCCTCTGTAAGGTGC		
EMD		F	GCCAGTACAACATCCCACAC	NM_203361.1	155
		R	CGCCGAATCTAAGTCCGAGA		

[1]*CYP7A1* = cholesterol 7alpha-hydroxylase; *HSD3B7* = 3 beta-hydroxysteroid dehydrogenase type 7; *CYP8B1* = sterol 12-alpha-hydroxylase; *AKR1D1* = aldo-keto reductase family 1 member D1; *CYP27A1* = sterol 27-hydroxylase; *CYP7B1* = oxysterol 7-alpha-hydroxylase; *CH25H* = cholesterol 25-hydroxylase; *CYP46A1* = cholesterol 24-hydroxylase; *BAAT* = bile acid coenzyme A:amino acid N-acyltransferase; *NTCP*, *SLC10A1* = Na^+-taurocholate cotransporting polypeptide; *SLC10A2*, *ASBT* = apical sodium-dependent bile acid transporter; *OSTα*, *SLC51A1* = solute carrier family 51 subunit α; *OSTβ*, *SLC51B* = solute carrier family 51 subunit β; *MRP2*, *ABCC2* = multidrug resistance-associated protein; *MDR1*, *ABCB1* = multidrug resistance protein 1; *BSEP*, *ABCB11* = bile salt export pump; *MDR3*, *ABCB4* = multiple drug resistance 3; *FXR*, *NR1H4* = farnesoid X receptor; *TGR5*, *GPBAR1* = Takeda G protein-coupled receptor 5; *NR1I2*, *PXR* = nuclear receptor subfamily 1, group I, member 2; *S1PR2* = sphingosine-1-phosphate receptor 2; *VDR* = vitamin D receptor; *CHRM2* = cholinergic receptor muscarinic 2; *RXRα*, *NR2B1* = retinoid X receptor alpha; *SHP1* = small heterodimer partner; *CAR* = constitutive androstane receptor; *YWHAZ* = tyrosine 3-monooxygenase/tryptophan 5-monooxygenase activation protein zeta; *EIF3K* = eukaryotic translation initiation factor 3 subunit K; *HPCAL1* = hippocalcin-like 1; *POLR2A* = RNA polymerase II subunit A; *GAPDH* = glyceraldehyde-3-phosphate dehydrogenase; *MARVELD1* = MARVEL domain containing 1; *LRP10* = LDL receptor related protein 10; *EMD* = emerin.

[2]F = forward; R = reverse.

were measured in triplicates using the Biomark HD RT-qPCR system and 96.96 integrated fluidic circuits (**IFC**). Preparation of the IFC was performed according to the protocol "Fast Gene Expression Analysis Using EvaGreen on Biomark HD or Biomark" from Fluidigm. To compensate for variations between IFC, 3 inter-run calibrators were added to each IFC. For subsequent gene expression analysis, the Biomark HD real-time PCR reader was used with the protocol "GE Fast 96 × 96 PCR + Meltv2."

Quality control of the melting and amplification curves was performed using Fluidigm real-time PCR Analysis Software (ver. 4.5.2). Inter-run calibration was performed using qBASE^{plus} software (ver. 3.3, Biogazelle, Ghent, Belgium). Differences in the quantification cycle between the inter-run calibrators of the runs were compared, and corrections or calibration factors were determined to compensate for the differences between runs. Three reference genes were determined by GeNormPlus (included in qBASE^{plus}) to serve as optimal numbers for normalization (i.e., *EIF3K*, *LRP10*, and *POLR2A*). Reference genes were determined as described in detail by Alaedin et al. (2021). The normalized values were used for statistical analysis of the mRNA data.

Statistical Analyses

Statistical analyses of BA concentrations in blood and scAT as well as mRNA abundance of BA-associated enzymes, receptors, and transporters were performed using a linear mixed model with repeated measures (IBM SPSS ver. 28). The model consisted of group, time, and interaction of group and time as fixed effects and cow as the random effect. Time was classified as repeated measures. Different variance–covariance structures were tested to determine the most appropriate variance–covariance structure. An autoregressive type 1 covariance structure and an identity covariance structure (scaled identity matrix) were selected as the best fit based on the Akaike and Bayesian information criteria. Bonferroni's correction was used to perform multiple comparisons. All residuals were tested for normality using the Kolmogorov–Smirnov test. Data that did not meet the assumptions of normality of residuals had to be log-transformed (base 10). Data were back-transformed for the figures and tables (mean ± SEM). Relationships between BA in serum and scAT were calculated by Spearman correlation using nontransformed data and represented by a heat map generated using JASP ver. 0.17.1 (JASP Team, 2019). Correlations between mRNA abundance of BA-related enzymes, transporters, and receptors were calculated only for the data analyzed under the mixed model. Correlation coefficients were considered as very strong ($1.0 \geq r \geq 0.9$), strong ($0.9 > r \geq 0.7$), moderate ($0.7 > r \geq 0.5$), weak ($0.5 > r \geq 0.3$), and very weak to zero correlation ($r < 0.3$). The threshold of significance was set at $P \leq 0.05$; trends were declared at $0.05 < P \leq 0.10$.

RESULTS

BA Concentrations in Serum

A total of 6 primary and 9 secondary BA, including their conjugates, were evaluated in serum. The mean percentage of each BA relative to the total BA in serum is shown in Figure 2A. In serum, CA and its conjugated

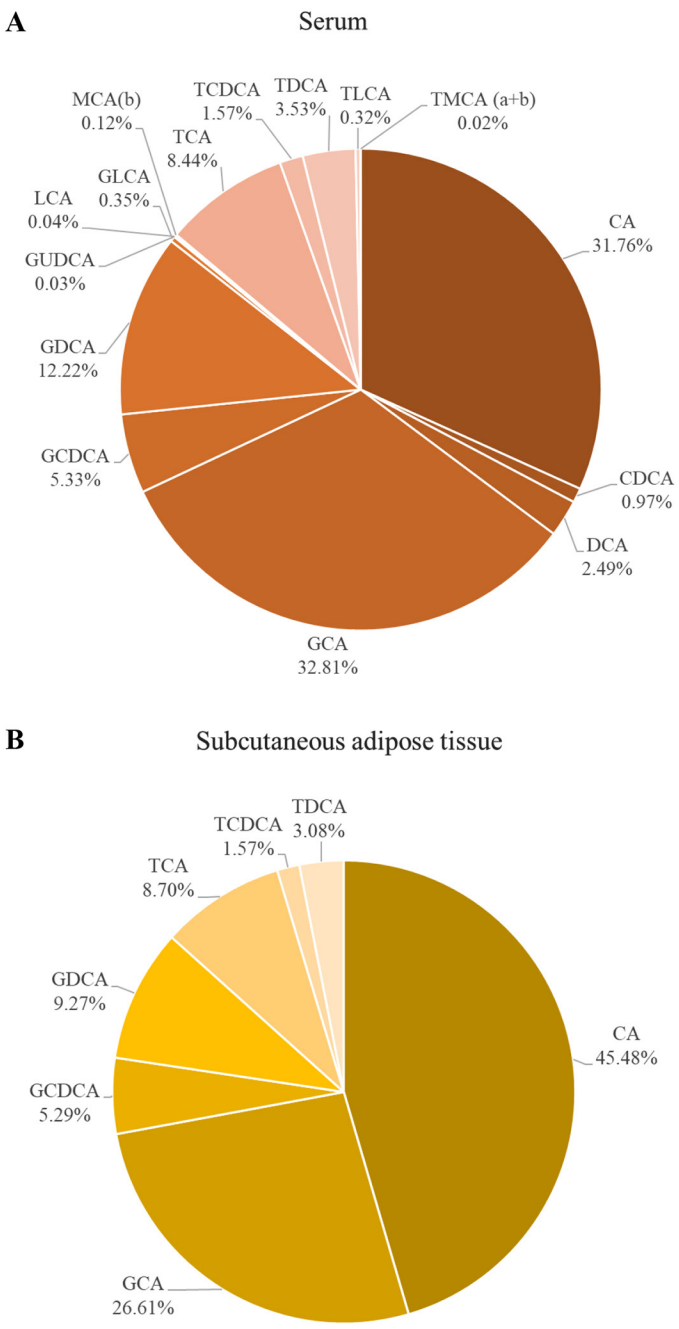

Figure 2. Mean percentage (%) of total bile acids in serum (A) and subcutaneous adipose tissue (B). Bile acids: cholic acid (CA), chenodeoxycholic acid (CDCA), taurocholic acid (TCA), glycocholic acid (GCA), taurochenodeoxycholic acid (TCDCA), glycochenodeoxycholic acid (GCDCA), deoxycholic acid (DCA), lithocholic acid (LCA), taurodeoxycholic acid (TDCA), glycodeoxycholic acid (GDCA), taurolithocholic acid (TLCA), glycolithocholic acid (GLCA), glycoursodeoxycholic acid (GUDCA), tauroursodeoxycholic acid (TUDCA), tauromuricholic acid (TMCA [a+b]), and β-muricholic acid (MCA[b]).

form GCA account for the largest proportion of the total BA (approximately 65%). The concentrations of BA in serum from wk 7 a.p. to wk 12 p.p. are shown in Figure 3. The concentration of serum BA changed over time, except for GLCA. For CA, CDCA, TCA, GCA, GCDCA, DCA, and β-muricholic acid concentrations were greater after calving than a.p. Regardless of time, concentrations of CA, CDCA, GCA, DCA, GCDCA, TCA, LCA, and GDCA were greater ($P \leq 0.05$) in NBCS cows than in HBCS cows.

BA Concentrations in scAT

A total of 5 primary and 2 secondary BA were detected in scAT. The average percentages of each BA relative to the total BA in scAT are shown in Figure 2B. In scAT, CA and its conjugated form GCA had the highest proportion of the total BA. The concentrations of BA in scAT from wk 7 a.p. to wk 12 p.p. are presented in Figure 4. The concentrations of CA, GDCA, and GCA were lower ($P \leq 0.001$) before calving and at wk 1 p.p. compared with wk 3 and 12 p.p. In addition, GCDCA concentrations a.p. were lower compared with p.p. concentrations ($P \leq 0.001$). Across all time points, higher concentrations of GCA (1.46-fold, $P \leq 0.001$), GCDCA (1.40-fold, $P \leq 0.001$), GDCA (1.63-fold, $P \leq 0.001$), TDCA (1.19-fold, $P = 0.02$), and TCDCA (1.35-fold, $P = 0.01$) were measured in NBCS cows compared with HBCS cows. At wk 3 p.p., an interaction ($P = 0.01$) between group and time was observed in CA concentrations, with NBCS cows showing 2.4 times higher ($P \leq 0.001$) CA levels than HBCS cows, indicating a time-specific differential response between the groups.

Relationship Between BA in Serum and scAT

The correlations between BA in serum and scAT are shown in Figure 5. Glycine-conjugated BA in serum and scAT were weakly correlated, with correlation coefficients ranging from r = 0.447 to 0.498. Significant positive correlations between taurine-conjugated BA in serum and scAT ranged from r = 0.276 to 0.356. Serum CA was positively associated with CA as well as with glycine-conjugated BA (i.e., GCA, GCDCA, and GDCA; $P \leq 0.001$) in scAT.

mRNA Abundance of BA-Related Enzymes in scAT

The mRNA abundance of enzymes related to the BA metabolism in scAT is shown in Table 2. In HBCS cows, the mRNA abundance of 3 β-hydroxysteroid dehydrogenase type 7 (*HSD3B7*) was 1.53-fold higher at 3 wk p.p. ($P \leq 0.001$) and 1.41-fold higher at 12 wk p.p. ($P = 0.02$) compared with NBCS cows. An interaction between group and time was observed for the mRNA abundance of cholesterol-24S-hydroxylase (*CYP46A1*; $P = 0.04$), with HBCS cows having a 2.16-fold higher

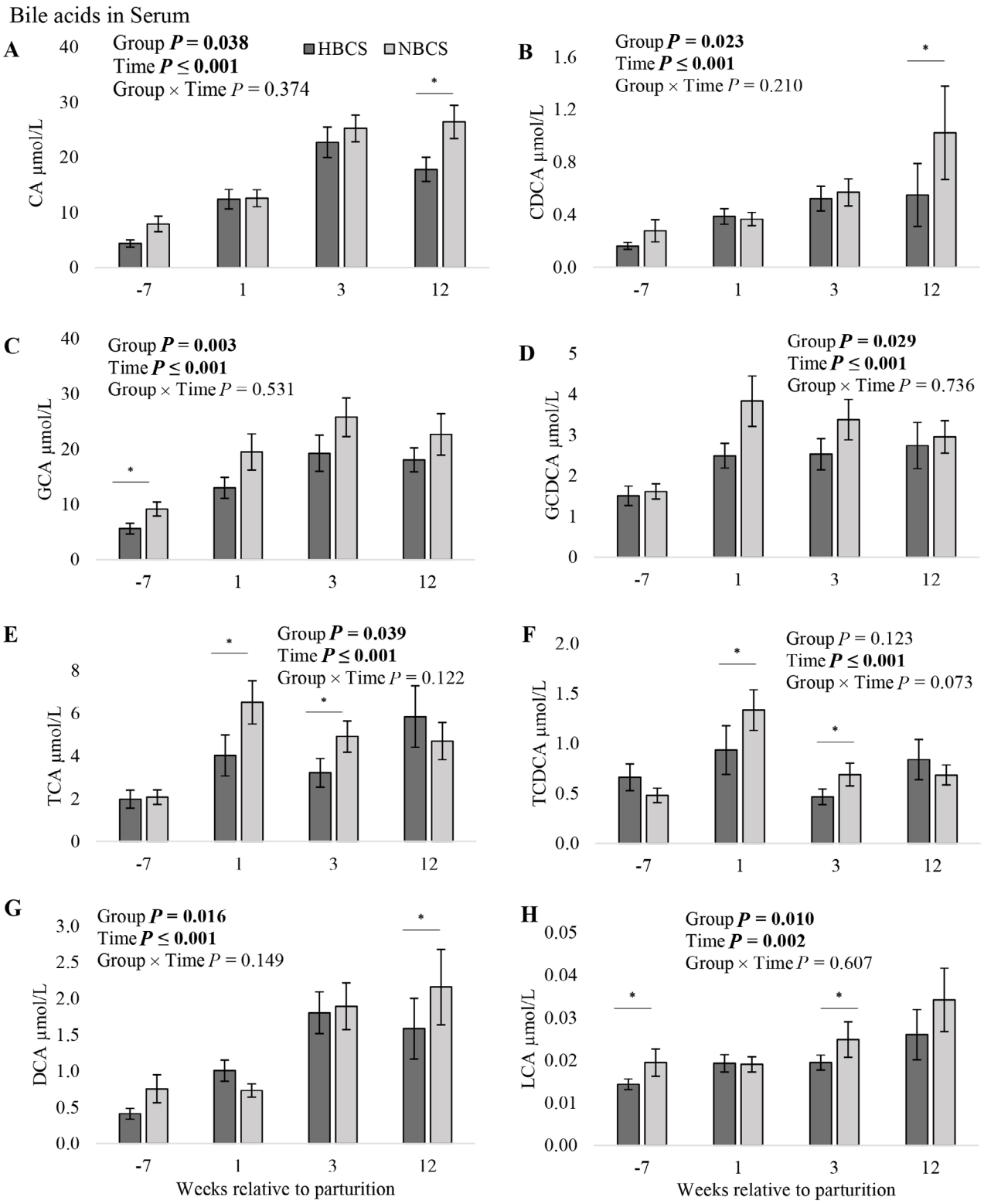

Figure 3. Concentration of bile acids (µmol/L) in serum from cows with normal (NBCS) versus high BCS (HBCS) at wk −7 antepartum and wk 1, 3, and 12 postpartum. Values are given as means ± SEM. Significant differences ($P \leq 0.05$) between the groups are indicated by asterisks. (A) Cholic acid (CA), (B) chenodeoxycholic acid (CDCA), (C) glycocholic acid (GCA), (D) glycochenodeoxycholic acid (GCDCA), (E) taurocholic acid (TCA), (F) taurochenodeoxycholic acid (TCDCA), (G) deoxycholic acid (DCA), (H) lithocholic acid (LCA), (I) glycodeoxycholic acid (GDCA), (J) glycolithocholic acid (GLCA), (K) taurodeoxycholic acid (TDCA), (L) taurolithocholic acid (TLCA), (M) β-muricholic acid (MCA[b]), (N) sum of α- and β-tauromuricholic acid (TMCA[a+b]), and (O) glycoursodeoxycholic acid (GUDCA). Significant *P*-values are shown in bold.

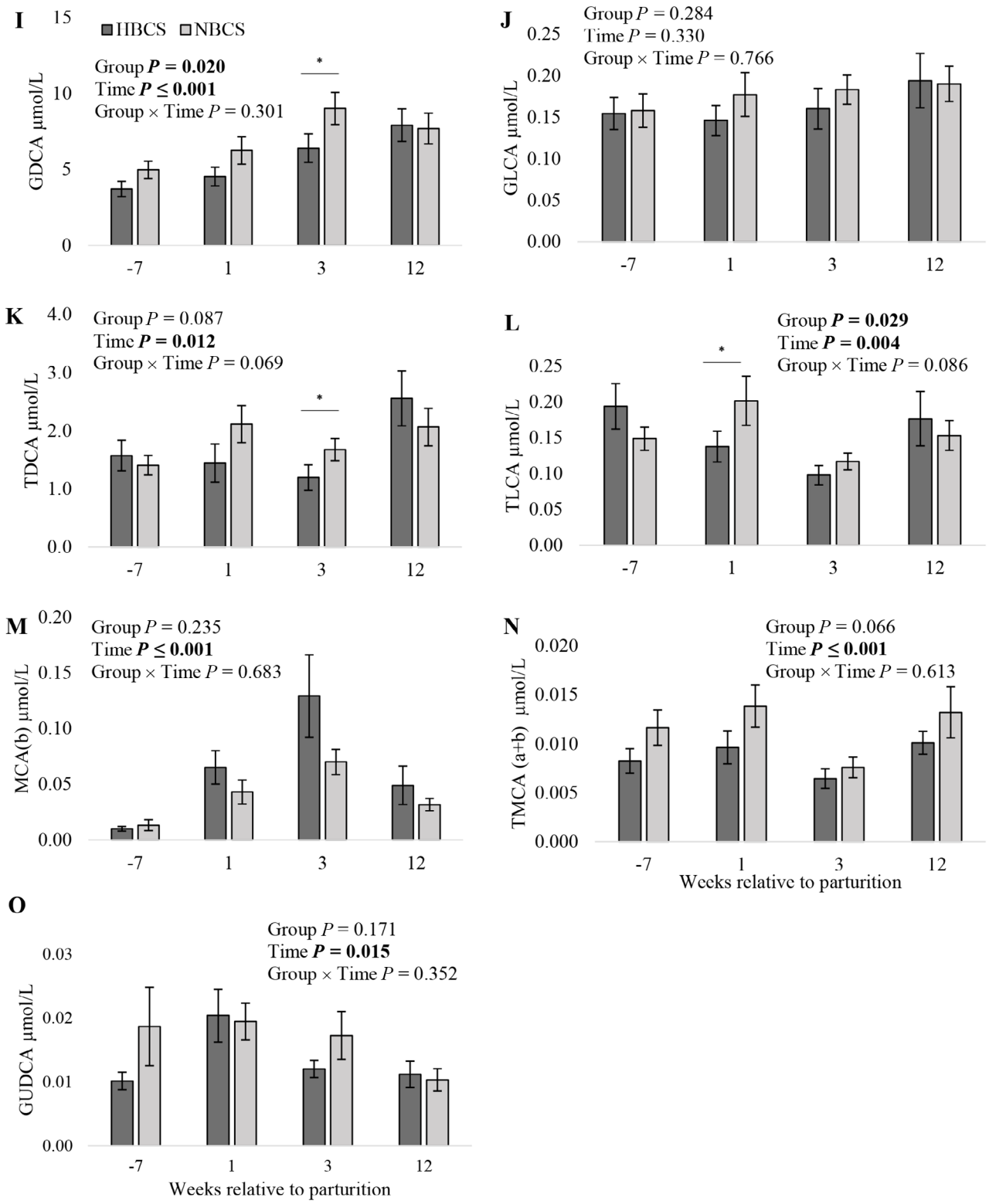

Figure 3 (Continued). Concentration of bile acids (µmol/L) in serum from cows with normal (NBCS) versus high BCS (HBCS) at wk −7 antepartum and wk 1, 3, and 12 postpartum. Values are given as means ± SEM. Significant differences ($P \leq 0.05$) between the groups are indicated by asterisks. (A) Cholic acid (CA), (B) chenodeoxycholic acid (CDCA), (C) glycocholic acid (GCA), (D) glycochenodeoxycholic acid (GCDCA), (E) taurocholic acid (TCA), (F) taurochenodeoxycholic acid (TCDCA), (G) deoxycholic acid (DCA), (H) lithocholic acid (LCA), (I) glycodeoxycholic acid (GDCA), (J) glycolithocholic acid (GLCA), (K) taurodeoxycholic acid (TDCA), (L) taurolithocholic acid (TLCA), (M) β-muricholic acid (MCA[b]), (N) sum of α- and β-tauromuricholic acid (TMCA[a+b]), and (O) glycoursodeoxycholic acid (GUDCA). Significant *P*-values are shown in bold.

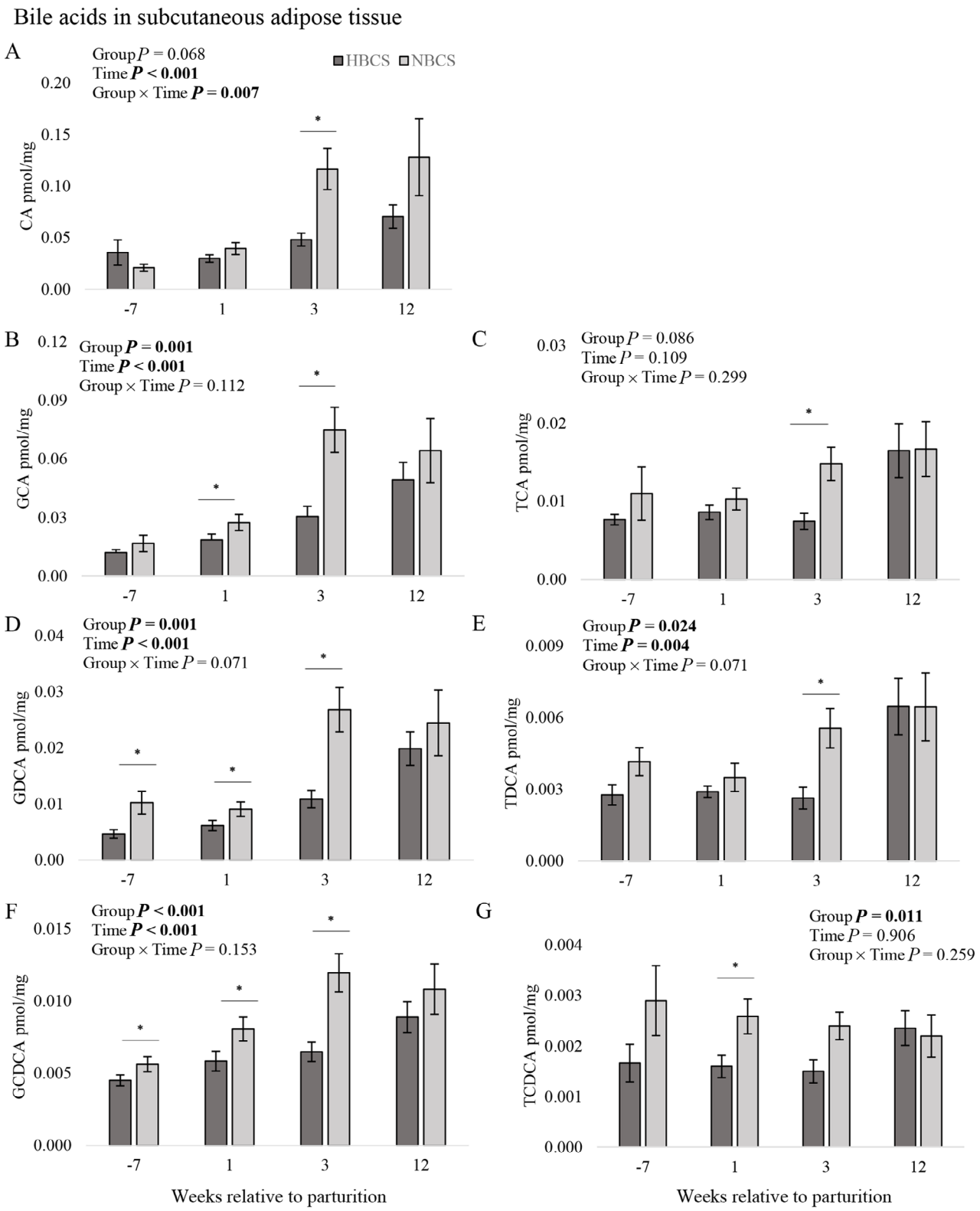

Figure 4. Concentration of bile acids (pmol/ng) in subcutaneous adipose tissue from cows with normal (NBCS) versus high body condition score (HBCS) at wk −7 antepartum and wk 1, 3, and 12 postpartum. Values are given as means ± SEM. Significant differences ($P \leq 0.05$) between the groups are indicated by asterisks. (A) Cholic acid (CA), (B) glycocholic acid (GCA), (C) taurocholic acid (TCA), (D) glycodeoxycholic acid (GDCA), (E) taurodeoxycholic acid (TDCA), (F) glycochenodeoxycholic acid (GCDCA), (G) taurochenodeoxycholic acid (TCDCA). Significant *P*-values are shown in bold.

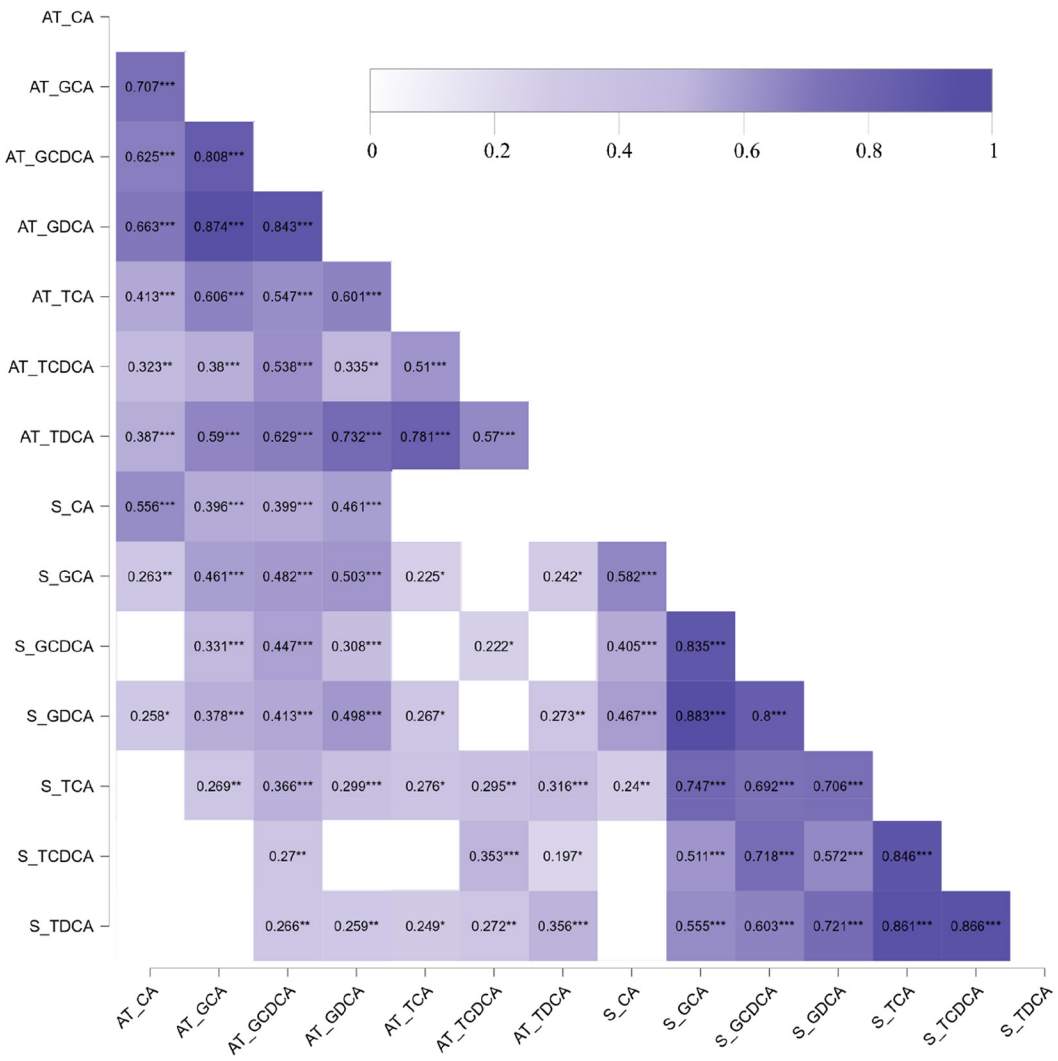

Figure 5. Correlations between serum (S) bile acids and subcutaneous adipose tissue (AT) bile acids independent of group and time. Bile acids: cholic acid (CA), glycocholic acid (GCA), taurocholic acid (TCA), glycodeoxycholic acid (GDCA), taurodeoxycholic acid (TDCA), glycochenodeoxycholic acid (GCDCA), and taurochenodeoxycholic acid (TCDCA). Asterisks indicate significant differences: *$P \leq 0.05$, **$P \leq 0.01$, ***$P \leq 0.001$.

($P = 0.01$) mRNA abundance than NBCS cows at wk 7 a.p. Furthermore, in HBCS cows, the mRNA abundance of *CYP46A1* was higher before calving compared with wk 3 p.p. (3.76-fold; $P \leq 0.001$).

Relationship Between BA and the mRNA Abundance of BA-Related Enzymes in scAT

Before parturition, the mRNA abundance of sterol 27-hydroxylase (*CYP27A1*) was negatively correlated with GDCA (r = −0.34, $P \leq 0.05$). Moreover, negative correlations were observed between the mRNA abundance of *CYP46A1* and GDCA at wk 7 a.p. (r = −0.34, $P \leq 0.05$), as well as TCDCA (r = −0.42, $P \leq 0.05$) and TDCA (r = −0.43, $P \leq 0.05$), both at wk 1 p.p. At wk 1 p.p., the mRNA abundance of cholesterol 25-hydroxylase (*CH25H*) was positively associated with GCDCA (r = 0.37, $P \leq 0.05$), TCDCA (r = 0.59, $P \leq 0.01$), TDCA (r = 0.49, $P \leq 0.05$) and between the mRNA abundance of *CH25H* and GCDCA at wk 12 p.p. (r = 0.42, $P \leq 0.05$).

BA Transporters in scAT

The mRNA abundance of BA transporters in scAT is shown in Table 3. The mRNA abundance of the apical sodium-dependent BA transporter (*ASBT/SLC10A2*) and the organic solute transporters (*OST-α/SLC51A1*) were not detectable in scAT. Irrespective of grouping, the mRNA abundances of the Na^+-taurocholate cotransporting polypeptide (*NTCP*/SLC10A1) were higher a.p.

Table 2. mRNA abundance of enzymes related to bile acid metabolism in subcutaneous adipose tissue from cows with normal (NBCS) and high BCS (HBCS) at wk 7 antepartum and at wk 1, 3, and 12 postpartum

	Week relative to parturition								*P*-value		
	−7		1		3		12				
Gene[1]	HBCS	NBCS	HBCS	NBCS	HBCS	NBCS	HBCS	NBCS	Group	Time	Group × time
CYP7A1											
Mean	0.002	0.001	0.000	0.001	0.002	0.009	—	0.001	—	—	—
SEM	0.001	0.000				0.007	—				
N	3	4	1	1	1	2	—	1			
HSD3B7											
Mean	1.034	1.212	1.384	0.906	1.440	1.463	1.951	1.384	0.008*	0.009*	0.067
SEM	0.092	0.268	0.161	0.107	0.191	0.216	0.273	0.181			
N	19	17	18	19	17	16	16	11			
CYP8B1											
Mean	0.159	0.269	0.545	0.483	0.262	0.434	0.555	0.423	0.250	<0.001*	0.268
SEM	0.036	0.067	0.125	0.133	0.046	0.079	0.178	0.055			
N	11	13	12	10	12	8	10	7			
AKR1D1											
Mean	0.010	0.004	0.002	0.008	0.002	0.012	0.001	—	—	—	—
SEM	0.004	0.001	0.000	0.004	0.000	0.010	0.000	—			
N	8	13	2	8	6	6	2	—			
CYP27A1											
Mean	0.376	0.341	0.335	0.340	0.342	0.318	0.336	0.392	0.832	0.714	0.643
SEM	0.035	0.024	0.032	0.029	0.027	0.029	0.026	0.050			
N	19	17	19	19	17	16	17	11			
CYP7B1											
Mean	0.388	0.287	0.589	0.471	0.795	0.684	0.943	0.648	0.309	<0.001*	0.897
SEM	0.089	0.043	0.108	0.067	0.182	0.078	0.224	0.142			
N	12	12	11	10	8	4	7	4			
CH25H											
Mean	0.785	0.894	1.742	3.359	1.570	2.324	2.250	2.668	0.038*	<0.001*	0.982
SEM	0.194	0.153	0.409	1.472	0.447	0.483	0.423	0.563			
N	18	16	15	17	16	15	17	11			
CYP46A1											
Mean	4.282	1.986	1.878	2.194	1.138	1.301	1.473	1.163	0.363	<0.001*	0.039*
SEM	0.653	0.287	0.425	0.354	0.216	0.205	0.207	0.238			
N	19	17	17	18	15	11	14	10			
BAAT											
Mean	0.737	0.541	0.672	0.772	0.711	0.566	0.488	0.719	0.903	0.779	0.095
SEM	0.112	0.070	0.115	0.119	0.090	0.081	0.082	0.114			
N	14	15	15	17	13	11	12	10			

[1]*CYP7A1* = cholesterol 7alpha-hydroxylase; *CYP27A1* = sterol 27-hydroxylase; *HSD3B7* = 3 beta-hydroxysteroid dehydrogenase type 7; *CYP8B1* = sterol 12-alpha-hydroxylase; *AKR1D1* = aldo-keto reductase family 1 member D1; *CH25H* = cholesterol 25-hydroxylase; *CYP46A1* = cholesterol 24-hydroxylase; *BAAT* = bile acid coenzyme A:amino acid N-acyltransferase; *CYP7B1* = oxysterol 7-alpha-hydroxylase. N: number.

*Statistically significant ($P \leq 0.05$) values indicated with an asterisk.

when compared with wk 1, 3, and 12 p.p. (3.71-, 4.81-, and 3.82-fold, respectively; all $P \leq 0.001$). An interaction between group and time was observed for the mRNA abundance of *NTCP*, with 2.52-fold higher mRNA abundance in HBCS compared with NBCS cows before calving ($P \leq 0.001$).

Relationship Between BA and the mRNA Abundance of BA-Related Transporters in scAT

The mRNA abundance of *NTCP* and GDCA were negatively correlated at wk 7 a.p. (r = −0.36; $P \leq 0.05$). Regarding wk 1 p.p., the mRNA abundance of the bile salt export pump (*BSEP*) was negatively correlated with all scAT BA except CA (GCA, r = −0.62, $P \leq 0.05$; GCDCA, r = −0.61, $P \leq 0.01$; GDCA, r = −0.55, $P \leq 0.05$; TCA, r = −0.80, $P \leq 0.01$; TCDCA, r = −0.78, $P \leq 0.01$; and TDCA, r = −0.67, $P \leq 0.01$). Furthermore, the mRNA abundance of the multidrug resistance protein 1 (*MDR1*) was negatively correlated with the glycine-conjugated BA GCA (r = −0.34; $P \leq 0.05$) and GCDCA (r = −0.46; $P \leq 0.01$) at wk 1 p.p. In addition, the mRNA abundance of *MDR1* was negatively correlated with CA (r = −0.54; $P \leq 0.01$), GCA (r = −0.52; $P \leq 0.01$), GDCA (r = −0.55; $P \leq 0.001$), and TDCA (r = −0.50; $P \leq 0.001$) at wk 3 p.p., whereas at wk 12 p.p., the mRNA abundance of *MDR1* was negatively correlated with CA (r = −0.51; $P \leq 0.01$), GCA (r = −0.67; $P \leq 0.001$), GCDCA (r = −0.58;

Table 3. mRNA abundance of transporters related to bile acid metabolism in subcutaneous adipose tissue from cows with normal (NBCS) and high BCS (HBCS) at wk 7 antepartum and at wk 1, 3, and 12 postpartum

	Week relative to parturition								*P*-value		
	−7		1		3		12				
Gene[1]	HBCS	NBCS	HBCS	NBCS	HBCS	NBCS	HBCS	NBCS	Group	Time	Group × time
NTCP (gene: *SLC10A1*)											
Mean	0.136	0.054	0.016	0.033	0.011	0.034	0.018	0.034	0.297	<0.001*	<0.001*
SEM	0.019	0.015	0.004	0.007	0.001	0.021	0.003	0.012			
N	18	17	11	15	13	8	12	10			
OSTβ (gene: *SLC51B*)											
Mean	0.005	—	0.003	0.024	—	0.014	—	0.009	—	—	—
SEM	0.003	—		0.017	—		—	0.001			
N	3	—	1	3	—	1	—	3			
MRP2 (gene: *ABCC2*)											
Mean	0.008	0.005	0.006	0.010	0.003	0.015	0.006	0.005	—	—	—
SEM	0.003	0.002	0.002	0.005	0.000	0.011	0.001	0.004			
N	8	10	6	6	6	5	5	2			
MDR1 (gene: *ABCB1*)											
Mean	1.637	1.997	2.097	2.171	2.419	2.045	1.658	1.830	0.838	0.001*	0.135
SEM	0.153	0.289	0.198	0.202	0.239	0.227	0.255	0.207			
N	19	17	19	19	17	16	16	11			
BSEP (gene: *ABCB11*)											
Mean	0.012	0.009	0.013	0.014	0.012	0.021	0.017	0.013	0.930	0.229	0.104
SEM	0.003	0.001	0.003	0.003	0.004	0.007	0.005	0.001			
N	9	14	6	12	10	7	5	4			
MDR3 (gene: *ABCB4*)											
Mean	1.399	0.869	1.615	1.419	—	1.612	1.523	2.614	—	—	—
SEM	0.690	0.464	1.161	1.204	—	—	1.378	1.262			
N	3	3	3	3	—	1	3	2			

[1]*NTCP*, *SLC10A1* = Na^+-taurocholate cotransporting polypeptide; *OSTβ*, *SLC51B* = solute carrier family 51 subunit β; *MRP2*, *ABCC2* = multidrug resistance-associated protein; *MDR1*, *ABCB1* = multidrug resistance protein 1; *BSEP*, *ABCB11* = bile salt export pump; *MDR3*, *ABCB4* = multiple drug resistance 3. N: number.

*Statistically significant ($P \leq 0.05$) values indicated with an asterisk.

$P \leq 0.01$), GDCA (r = −0.63; $P \leq 0.001$), TCA (r = −0.52; $P \leq 0.01$), TCDCA (r = −0.49; $P \leq 0.05$), TDCA (r = −0.48; $P \leq 0.05$) in scAT.

BA Receptors in scAT

The mRNA abundance of BA receptors in scAT is shown in Table 4. The mRNA abundance of *TGR5* and cholinergic receptor muscarinic 2 (*CHRM2*) were up to 3.70- and 4.13-fold higher ($P \leq 0.001$) at wk 3 p.p. compared with a.p. Moreover, the mRNA abundance of the retinoid X receptor α (*RXRα*; *NR2B1*) was highest at wk 12 p.p. compared with all other time points ($P \leq 0.001$). Regarding group differences, the mRNA abundance of *S1PR2* was 2.12-fold ($P = 0.04$) higher in NBCS cows than in HBCS cows.

DISCUSSION

Synthesized from cholesterol, BA are known to affect metabolic processes such as lipid and glucose metabolism as well as general energy homeostasis (Shapiro et al., 2018). In the periparturient period, the metabolism of high-yielding dairy cows is challenged by calving and the onset of lactation. Overconditioned cows, mobilizing more body reserves, are more susceptible to metabolic disorders compared with thinner cows (Bernabucci et al., 2005). In the present study, increased mobilization of AT in HBCS cows was indicated by higher nonesterified fatty acids concentrations as well as the loss of BFT and BCS in HBCS cows compared with NBCS cows after parturition (Schuh et al., 2019; Supplemental Figures S1, S2, and S5, see Notes). Excessive lipolysis in overconditioned dairy cows, knowingly affected plasma BA and activated secondary BA biosynthesis in the gut microbiome (Gu et al., 2023). In our study, cows with different body conditions around calving had different serum and scAT BA profiles, with increasing serum BA concentrations at the onset of lactation. In the current study, CA and GCA were the dominant BA in serum and scAT, as reported in ruminants (Sheriha et al., 1968; Washizu et al., 1991; Reiter et al., 2021). Postprandial stimuli are known to affect BA synthesis in the liver, BA circulation in enterohepatic tissues, and serum (LaRusso et al., 1978; Hofmann, 1999). Herein we assumed, that higher p.p. BA concentrations in serum might be related to increasing DMI after parturition. However, the relationship between serum BA and DMI (an increase in DMI was previously reported by Schuh et al., 2019; Supplemental Figure S3, see Notes) was limited to a few BA at wk 1 p.p. (i.e., TCA, TCDCA, TMCA, GDCA, and TDCA; data not shown). In dairy cows, most serum levels of BA change during the dry period and lactation (Ghaffari et al., 2024). The increasing metabolic demand for milk synthesis associated with dietary changes resulted in increased BA synthesis to facilitate digestion and absorption of dietary lipids (Ghaffari et al., 2024). In humans, the body mass index was positively correlated with BA concentrations in the fasting period (Prinz et al., 2015) and negatively correlated with postprandial BA concentrations (Brufau et al., 2010). Moreover, obesity suppressed the normal postprandial increase in circulating BA (Ahmad et al., 2013; Haeusler et al., 2016). Given that excessive lipolysis 7 d after calving altered the gut microbiota in transition cows, leading to changes in the composition of secondary BA (Gu et al., 2023), it may suggest that the lower serum BA concentrations in HBCS cows compared with NBCS cows might be due to higher fecal BA excretion.

In the present study, we observed 7 BA in scAT using a targeted metabolomics approach via LC-ESI-MS /MS that allowed detection of 20 BA. Because both primary and secondary BA, as well as their conjugates, were present in scAT, we assume that BA can be taken up from circulation into scAT. The trend toward lower concentrations of BA in scAT before calving and increasing concentrations after the onset of lactation were consistent with higher circulating BA concentrations after parturition. However, the weak-to-moderate correlations between BA in serum and in scAT were not adequate to indicate clear bioactive mechanisms. In bovine estrus, very strong relationships between serum and follicular fluid CA (up to r = 0.97; $P \leq 0.001$) indicated predominant diffusion of circulating CA across the follicular membrane (Blaschka et al., 2020). The relationship was stronger for glycine-conjugated BA than for taurine-conjugated BA. The moderate correlation between CA in serum and scAT may indicate the ability of CA to cross cell membranes by passive diffusion, whereas transport of conjugated BA into cells depends on specific transporters (Hofmann, 1999). Because secondary BA are synthesized exclusively by the gut microbiome (Chiang, 2015), de novo synthesis in scAT seems unlikely. Furthermore, the tissue-specific conjugation patterns of BA as well as the specific expression of BA transporters suggest selective uptake of conjugated BA in peripheral tissues such as serum, kidney, and heart (Swann et al., 2011). The mRNA abundance of BA transporters, that is, the mRNA abundance of *NTCP* and *BSEP*, being mainly responsible for the import and export of BA within the liver (Trauner and Boyer, 2003), were detectable in scAT from dairy cows in the present study. In mouse adipocyte cell culture, expression of *BSEP* mRNA and export of BA from cells to the circulation via BSEP appeared to be essential for preventing cytotoxic accumulation of BA within cells (Schmid et al., 2019). Whether this also applies for AT from dairy cows has not been investigated thus far. However, the negative moderate correlations at wk 1 p.p. with all conjugated BA, led to the assumption

Table 4. mRNA abundance of receptors related to bile acid metabolism in subcutaneous adipose tissue from cows with normal (NBCS) and high BCS (HBCS) at wk 7 antepartum and wk 1, 3, and 12 postpartum

	Week relative to parturition								*P*-value		
	−7		1		3		12				
Gene[1]	HBCS	NBCS	HBCS	NBCS	HBCS	NBCS	HBCS	NBCS	Group	Time	Group × time
FXR (gene: *NR1H4*)											
Mean	0.001	0.006	—	0.004	0.006	—	—	—	—	—	—
SEM	0.000	0.003	—	—	—	—	—	—			
N	3	3	—	1	1	—	—	—			
TGR5 (gene: *GPBAR1*)											
Mean	0.102	0.113	0.312	0.285	0.374	0.419	0.273	0.340	0.462	<0.001*	0.908
SEM	0.032	0.026	0.090	0.051	0.089	0.114	0.060	0.165			
N	11	10	11	12	9	10	9	3			
S1PR2 (gene: *S1PR2*)											
Mean	1.038	2.580	0.954	1.462	0.778	1.277	1.008	0.683	0.039*	0.276	0.121
SEM	0.338	1.085	0.254	0.492	0.114	0.170	0.246	0.051			
N	6	5	7	7	5	10	5	4			
VDR (gene: *VDR*)											
Mean	1.636	0.931	2.372	1.977	0.818	0.995	1.074	1.572	—	—	—
SEM	0.459	0.256	1.449	0.455	0.176	0.995	0.251	1.249			
N	5	8	4	6	5	4	6	2			
CHRM2 (gene: *CHRM2*)											
Mean	0.486	0.484	0.825	1.596	1.916	2.101	1.781	1.598	0.103	<0.001*	0.713
SEM	0.123	0.119	0.112	0.617	0.975	0.619	0.413	0.516			
N	16	13	16	15	15	14	16	11			
RXRα (gene: *NR2B1*)											
Mean	0.584	0.599	0.583	0.550	0.498	0.563	0.751	0.741	0.664	<0.001*	0.621
SEM	0.047	0.038	0.028	0.026	0.030	0.049	0.032	0.042			
N	19	17	19	19	17	16	16	11			
CAR (gene: *NR1I3*)											
Mean	0.007	0.003	0.005	0.006	0.002	0.017	—	—	—	—	—
SEM	0.003	0.001	0.002	0.001		0.011	—	—			
N	7	9	3	4	1	3	—	—			

[1]*FXR*, *NR1H4* = farnesoid X receptor; *TGR5*, *GPBAR1* = Takeda G protein-coupled receptor 5; *VDR* = vitamin D receptor; *S1PR2* = sphingosine-1-phosphate receptor 2; *CHRM2* = cholinergic receptor muscarinic 2; *RXRα*, *NR2B1* = retinoid X receptor alpha; *CAR* = constitutive androstane receptor. N: number.

*Statistically significant ($P \leq 0.05$) values indicated with an asterisk.

that BA might be eliminated from scAT through BSEP. As an adaptive regulation of BA entering into hepatocytes, *NTCP* gene expression is associated with the total hepatic BA concentration, thyroid and steroid hormones, cytokines, or injury in the liver (Alrefai and Gill, 2007; Geier et al., 2007; Dawson et al., 2009). Furthermore, BA indirectly regulate the expression of *NTCP* and *BSEP*, through the activation of signaling cascades via FXR, small heterodimer partner (**SHP**), and RXRα in humans and rodents (Anwer, 2004). As known in rats, FXR can bind BA, inducing the expression of *SHP*, and thus activating RXRα, which finally initiates NTCP (Jung et al., 2004). In the present study, the FXR mRNA abundance was below the limit of detection (**LOD**); however, the absence of mRNA does not definitely rule out FXR activity in general. Previous research, employing proteomic methods, has demonstrated substantial FXR pathway activity in AT in late-pregnant dairy cows (Zachut and Moallem, 2017). Because MDR1 does not exclusively transport BA (Klaassen and Aleksunes, 2010), the negative correlation between *MDR1* mRNA and BA after calving should be considered cautiously. MDR1 is responsible for the excretion of BA (Ayewoh and Swaan, 2022), organic cations, phospholipids (Anwer, 2004), and cholesterol from the liver into the bile (Honig et al., 2003). Therefore, transporters may depend on factors other than BA concentration in scAT.

The mRNA of key enzymes such as cholesterol 7α-hydroxylase (*CYP7A1*; Chiang and Ferrell, 2020) and aldo-keto reductase family 1 member D1 (*AKR1D1*; Chiang, 2004), being relevant for the de novo synthesis within the classical pathway, could only be detected in few samples below the LOD. However, oxysterol-7α -hydroxylase (*CYP7B1*), which is a marker enzyme of the alternative BA synthesis pathway (Chiang, 2017), was detected in scAT. Moreover, the weak-to-moderate negative correlations between the mRNA abundance of enzymes involved in the alternative pathway (*CYP27A1*, *CH25H*, and *CYP46A1*) and conjugated BA, point to a predominance of the alternative pathway. However, CDCA, the main BA of the alternative pathway, was detected below the LOD in scAT. Therefore, increasing mRNA abundance of *CYP7B1* throughout the experimental period might rather control cellular oxysterol concentrations as was recently reported in murine liver (Pandak and Kakiyama, 2019). Also, the cholesterol hydroxylase enzymes mRNA, *CH25H*, *CYP27A1*, and *CYP46A1*, generating oxysterols (Björkhem et al., 2002), have been detected in bovine scAT in this study. Oxysterols are precursors of BA (Russell, 2000), influencing lipid metabolism through activating the liver X receptor, which increases lipid synthesis by an induced expression of genes, such as sterol element binding protein-1c (*SREBP-1c*), FA synthase (*FAS*), stearoyl-CoA desaturase 1 (*SCD-1*), and acetyl-CoA carboxylase 1 (*ACC-1I*; Joseph et al., 2002; Talukdar and Hillgartner, 2006). In 3T3-L1 preadipocytes, oxysterol-forming enzymes (CYP27A1, CYP7B1) as well as oxysterols themselves, were synthesized (Li et al., 2014). Therefore, oxysterols might serve as an alternative way to metabolize cholesterol and thus protect adipocytes against cholesterol overload (Li et al., 2014). Catalysis of cholesterol to the oxysterol 25-hydroxycholesterol, CH25H, has been previously studied in obese humans, where weight reduction downregulated *CH25H* mRNA in the visceral AT (Dankel et al., 2010). In our study, HBCS cows that exhibited greater postpartum BCS loss than NBCS cows (Schuh et al., 2019) had lower mRNA abundance of *CH25H* than NBCS cows, suggesting a specific role for *CH25H* in lipid metabolism at least during periods of lipid mobilization. The higher mRNA abundance of *CYP46A1* in scAT of HBCS cows 7 wk before calving may indicate higher cholesterol degradation as described in human embryonic kidney 293 cells (Mast et al., 2003). The consistent abundance of *CYP27A1* mRNA across all time points irrespective of body condition suggests that this enzyme is of permanent importance in scAT. In addition to the formation of BA, CYP27A1 is also involved in the formation of oxysterol 27-hydroxycholesterol, which is formed de novo in adipocytes to protect against cholesterol overload (Li et al., 2014). Recently, the formation of oxysterols via the enzyme CYP27A1 was discussed in context with steroid biosynthesis in scAT of cows from the same study (Schuh et al., 2022).

Within the classical and alternative pathway of BA synthesis, HSD3B7 is involved in the production of CA and CDCA (Chiang, 2013; Li and Dawson, 2019); however, HSD3B7 serves as an important enzyme for the synthesis of oxysterols (Griffiths and Wang, 2019). Due to the lack of correlations between *HSD3B7* and BA, we assumed that HSD3B7 may be involved in oxysterol rather than BA synthesis in scAT. In addition, the higher mRNA abundance of *HSD3B7* in HBCS animals may point to the formation of oxysterols, which affects lipid metabolism (Russell, 2000). In addition, the present study detected the mRNA abundance of *BAAT* in scAT, the enzyme that conjugates BA in the liver (Falany et al., 1994). As postulated earlier, conjugation could protect adipocytes from cytotoxic BA overload (Monte et al., 2009).

In the present study, mRNA from both transmembrane (i.e., *TGR5*, *CHRM2*, and *S1PR2*) and nuclear BA receptors (*RXRα*) was present in scAT. The TGR5 is activated by BA concentrations (LCA, TLCA, CA, DCA, and CDCA) in the nanomolar range (Prawitt and Staels, 2010). In this study, CA could serve as the major ligand for TGR5 in scAT. Because ligand activation in AT and liver induced lipolysis and energy expenditure in mice and humans (Chávez-Talavera et al., 2017;

Velazquez-Villegas et al., 2018), the upregulation of mRNA abundance of *TGR5* with the onset of lactation could point to similar effects in dairy cows. Furthermore, although the mRNA abundance of *CHRM2* was detected in scAT, the concentrations of secondary BA DCA and LCA binding to CHRM2 (Evangelakos et al., 2021) in the present study were below the LOD. Moreover, albeit that GCDCA, GDCA, and TCDCA are not considered as potential agonists for CHRM2, the positive correlation between *CHRM2* and these BA may suggest a role as ligand precursor molecules (Xie et al., 2021). The S1PR2, a ubiquitously expressed G protein-coupled receptor (Adada et al., 2013) that serves as a receptor for sphingosine-1-phosphate and conjugated BA in liver (Wan and Sheng, 2018), was detected herein in scAT. As a ligand for S1PR2, TCA could regulate glucose and lipid metabolism as suggested in rodent hepatocytes (Studer et al., 2012). The nuclear receptor *RXRα*, being present in scAT, forms a heterodimer with FXR in the liver, which is activated via BA and subsequently prevents BA synthesis via inhibiting CYP7A1 (Lu et al., 2000). Bile acids are not direct ligands of the RXRα but bind to FXR (Jenkins and Hardie, 2008). Given that *FXR* mRNA was occasionally present in this study (with values below the LOD), the importance of the heterodimer formation (FXR and RXRα) is questionable.

CONCLUSIONS

Our study detects BA in serum and scAT of cows, as well as the mRNA abundance of BA-related enzymes, receptors, and transporters, suggesting a potential role of BA in lipid metabolism. Higher concentrations of BA in both serum and scAT after parturition may be associated with increasing DMI. Increasing lipid mobilization in overconditioned cows after parturition was accompanied by lower circulating BA concentrations. Conjugated BA may be actively transported from the circulation to the scAT via *NTCP* and exported via *BSEP* as well as metabolized by BA-related enzymes. Finally, the presence of specific BA receptors in scAT supports the potential role of BA in lipid metabolism during the periparturient period of dairy cows.

NOTES

H. Sadri received a Georg Forster Research Fellowship for experienced researchers, awarded by the Alexander von Humboldt Foundation (Bonn, Germany). The project was funded by the German Research Foundation (DFG, HA 6026/4-1; Bonn, Germany). The authors would like to acknowledge all coworkers at the Educational and Research Centre for Animal Husbandry, Hofgut Neumühle (Rhineland-Palatinate, Germany). We thank Inga Hofs (University of Bonn, Bonn, Germany) for supporting the mRNA analysis and Silke Becker, Julia Scarpa, and Werner Römisch-Margl (Metabolomics and Proteomics Core of the Helmholtz Zentrum München, Munich, Germany) for supporting the metabolomics measurements. Supplemental material for this article is available at https://doi.org/10.6084/m9.figshare.25843579. The trial was conducted following European regulations for the protection of experimental animals and was approved by the local authority for animal welfare affairs (Landesuntersuchungsamt Rheinland-Pfalz, Koblenz, Germany; G 14–20–071). The authors have not stated any conflicts of interest.

Nonstandard abbreviations used: a.p. = antepartum; AT = adipose tissue; BA = bile acids; BFT = back-fat thickness; CA = cholic acid; CAR = constitutive androstane receptor; CDCA = chenodeoxycholic acid; FXR = farnesoid X receptor; GCA = glycocholic acid; GCDCA = glycochenodeoxycholic acid; GDCA = glycodeoxycholic acid; GLCA = glycolithocholic acid; GUDCA = glycoursodeoxycholic acid; HBCS = high BCS; IFC = integrated fluidic circuits; LCA = lithocholic acid; LC-ESI-MS/MS = liquid chromatography-electrospray ionization-MS/MS; LOD = limit of detection; NBCS = normal BCS; p.p. = postpartum; RT-qPCR = quantitative reverse-transcription real-time PCR; scAT = subcutaneous AT; SHP = small heterodimer partner; S1PR2 = G protein-coupled sphingosine-1-phosphates receptor 2; TCA = taurocholic acid; TCDCA = taurochenodeoxycholic acid; TDCA = taurodeoxycholic acid; TGR5 = Takeda G protein-coupled receptor 5; TLCA = taurolithocholic acid; TMCA (a+b) = tauromuricholic acid (sum of α and β); VDR = vitamin D receptor.

REFERENCES

Adada, M., D. Canals, Y. A. Hannun, and L. M. Obeid. 2013. Sphingosine-1-phosphate receptor 2. FEBS J. 280:6354–6366. https://doi.org/10.1111/febs.12446.

Adewuyi, A. A., E. Gruys, and F. J. C. M. van Eerdenburg. 2005. Non esterified fatty acids (NEFA) in dairy cattle. A review. Vet. Q. 27:117–126. https://doi.org/10.1080/01652176.2005.9695192.

Ahmad, N. N., A. Pfalzer, and L. M. Kaplan. 2013. Roux-en-Y gastric bypass normalizes the blunted postprandial bile acid excursion associated with obesity. Int. J. Obes. (Lond.) 37:1553–1559. https://doi.org/10.1038/ijo.2013.38.

Alaedin, M., M. H. Ghaffari, H. Sadri, J. Meyer, S. Dänicke, J. Frahm, K. Huber, S. Grindler, S. Kersten, J. Rehage, E. Muráni, and H. Sauerwein. 2021. Effects of dietary l–carnitine supplementation on the response to an inflammatory challenge in mid-lactating dairy cows: Hepatic mRNA abundance of genes involved in fatty acid metabolism. J. Dairy Sci. 104:11193–11209. https://doi.org/10.3168/jds.2021-20226.

Alrefai, W. A., and R. K. Gill. 2007. Bile acid transporters: structure, function, regulation and pathophysiological implications. Pharm. Res. 24:1803–1823. https://doi.org/10.1007/s11095-007-9289-1.

Anwer, M. S. 2004. Cellular regulation of hepatic bile acid transport in health and cholestasis. Hepatology 39:581–590. https://doi.org/10.1002/hep.20090.

Armstrong, M. J., and M. C. Carey. 1982. The hydrophobic-hydrophilic balance of bile salts. Inverse correlation between reverse-phase high performance liquid chromatographic mobilities and micellar cholesterol-solubilizing capacities. J. Lipid Res. 23:70–80. https://doi.org/10.1016/S0022-2275(20)38175-X.

Ayewoh, E. N., and P. W. Swaan. 2022. Bile acid transporters. Pages 189–198 in Drug Transporters: Molecular Characterization and Role in Drug Disposition. 3rd ed. G. You and M. E. Morris, ed. John Wiley & Sons.

Bernabucci, U., B. Ronchi, N. Lacetera, and A. Nardone. 2005. Influence of body condition score on relationships between metabolic status and oxidative stress in periparturient dairy cows. J. Dairy Sci. 88:2017–2026. https://doi.org/10.3168/jds.S0022-0302(05)72878-2.

Björkhem, I., Z. Araya, M. Rudling, B. Angelin, C. Einarsson, and K. Wikvall. 2002. Differences in the regulation of the classical and the alternative pathway for bile acid synthesis in human liver. No coordinate regulation of CYP7A1 and CYP27A1. J. Biol. Chem. 277:26804–26807. https://doi.org/10.1074/jbc.M202343200.

Blaschka, C., A. Sánchez-Guijo, S. A. Wudy, and C. Wrenzycki. 2020. Profile of bile acid subspecies is similar in blood and follicular fluid of cattle. Vet. Med. Sci. 6:167–176. https://doi.org/10.1002/vms3.217.

Brufau, G., F. Stellaard, K. Prado, V. W. Bloks, E. Jonkers, R. Boverhof, F. Kuipers, and E. J. Murphy. 2010. Improved glycemic control with colesevelam treatment in patients with type 2 diabetes is not directly associated with changes in bile acid metabolism. Hepatology 52:1455–1464. https://doi.org/10.1002/hep.23831.

Chávez-Talavera, O., A. Tailleux, P. Lefebvre, and B. Staels. 2017. Bile acid control of metabolism and inflammation in obesity, type 2 diabetes, dyslipidemia, and nonalcoholic fatty liver disease. Gastroenterology 152:1679–1694.e3. https://doi.org/10.1053/j.gastro.2017.01.055.

Chen, Y.-S., H.-M. Liu, and T.-Y. Lee. 2019a. Ursodeoxycholic acid regulates hepatic energy homeostasis and white adipose tissue macrophages polarization in leptin-deficiency obese mice. Cells 8:253. https://doi.org/10.3390/cells8030253.

Chen, M. L., K. Takeda, and M. S. Sundrud. 2019b. Emerging roles of bile acids in mucosal immunity and inflammation. Mucosal Immunol. 12:851–861. https://doi.org/10.1038/s41385-019-0162-4.

Chiang, J. Y. L. 2004. Regulation of bile acid synthesis: pathways, nuclear receptors, and mechanisms. J. Hepatol. 40:539–551. https://doi.org/10.1016/j.jhep.2003.11.006.

Chiang, J. Y. L. 2009. Bile acids: Regulation of synthesis. J. Lipid Res. 50:1955–1966. https://doi.org/10.1194/jlr.R900010-JLR200.

Chiang, J. Y. L. 2013. Bile acid metabolism and signaling. Compr. Physiol. 3:1191–1212. https://doi.org/10.1002/cphy.c120023.

Chiang, J. Y. L. 2015. Negative feedback regulation of bile acid metabolism: impact on liver metabolism and diseases. Hepatology 62:1315–1317. https://doi.org/10.1002/hep.27964.

Chiang, J. Y. L. 2017. Recent advances in understanding bile acid homeostasis. F1000Research 6. https://doi.org/10.12688/f1000research.12449.1.

Chiang, J. Y. L., and J. M. Ferrell. 2020. Up to date on cholesterol 7 alpha-hydroxylase (CYP7A1) in bile acid synthesis. Liver Res. 4:47–63. https://doi.org/10.1016/j.livres.2020.05.001.

Dankel, S. N., D. J. Fadnes, A.-K. Stavrum, C. Stansberg, R. Holdhus, T. Hoang, V. L. Veum, B. J. Christensen, V. Våge, J. V. Sagen, V. M. Steen, and G. Mellgren. 2010. Switch from stress response to homeobox transcription factors in adipose tissue after profound fat loss. PLoS One 5:e11033. https://doi.org/10.1371/journal.pone.0011033.

Dawson, P. A., T. Lan, and A. Rao. 2009. Bile acid transporters. J. Lipid Res. 50:2340–2357. https://doi.org/10.1194/jlr.R900012-JLR200.

Di Ciaula, A., G. Garruti, R. Lunardi Baccetto, E. Molina-Molina, L. Bonfrate, D. Q.-H. Wang, and P. Portincasa. 2017. Bile acid physiology. Ann. Hepatol. 16:S4–S14. https://doi.org/10.5604/01.3001.0010.5493.

Drackley, J. K., H. M. Dann, N. Douglas, N. A. J. Guretzky, N. B. Litherland, J. P. Underwood, and J. J. Loor. 2005. Physiological and pathological adaptations in dairy cows that may increase susceptibility to periparturient diseases and disorders. Ital. J. Anim. Sci. 4:323–344. https://doi.org/10.4081/ijas.2005.323.

EMEA (European Medicines Agency). 2011. Guideline on bioanalytical method validation. EMEA/CHMP/EWP/192217/2009 Rev. 1 Corr. 2. EMEA Committee for Medicinal Products for Human Use, Amsterdam, the Netherlands.

Evangelakos, I., J. Heeren, E. Verkade, and F. Kuipers. 2021. Role of bile acids in inflammatory liver diseases. Semin. Immunopathol. 43:577–590. https://doi.org/10.1007/s00281-021-00869-6.

Falany, C. N., M. R. Johnson, S. Barnes, and R. B. Diasio. 1994. Glycine and taurine conjugation of bile acids by a single enzyme. Molecular cloning and expression of human liver bile acid CoA:amino acid N-acyltransferase. J. Biol. Chem. 269:19375–19379. https://doi.org/10.1016/S0021-9258(17)32178-6.

Ferrebee, C. B., and P. A. Dawson. 2015. Metabolic effects of intestinal absorption and enterohepatic cycling of bile acids. Acta Pharm. Sin. B 5:129–134. https://doi.org/10.1016/j.apsb.2015.01.001.

Geier, A., M. Wagner, C. G. Dietrich, and M. Trauner. 2007. Principles of hepatic organic anion transporter regulation during cholestasis, inflammation and liver regeneration. Biochim. Biophys. Acta Mol. Cell Res. 1773:283–308. https://doi.org/10.1016/j.bbamcr.2006.04.014.

Ghaffari, M. H., J. B. Daniel, H. Sadri, J. Martín-Tereso, and H. Sauerwein. 2024. Longitudinal characterization of the metabolome of dairy cows transitioning from one lactation to the next: Investigations in blood serum. J. Dairy Sci. 107:1263–1285. https://doi.org/10.3168/jds.2023-23841.

Griffiths, W. J., and Y. Wang. 2019. Oxysterol research: A brief review. Biochem. Soc. Trans. 47:517–526. https://doi.org/10.1042/BST20180135.

Gu, F., S. Zhu, Y. Tang, X. Liu, M. Jia, N. Malmuthuge, T. G. Valencak, J. W. McFadden, J.-X. Liu, and H.-Z. Sun. 2023. Gut microbiome is linked to functions of peripheral immune cells in transition cows during excessive lipolysis. Microbiome 11:40. https://doi.org/10.1186/s40168-023-01492-3.

Haeusler, R. A., S. Camastra, M. Nannipieri, B. Astiarraga, J. Castro-Perez, D. Xie, L. Wang, M. Chakravarthy, and E. Ferrannini. 2016. Increased bile acid synthesis and impaired bile acid transport in human obesity. J. Clin. Endocrinol. Metab. 101:1935–1944. https://doi.org/10.1210/jc.2015-2583.

Hofmann, A. F. 1999. The continuing importance of bile acids in liver and intestinal disease. Arch. Intern. Med. 159:2647–2658. https://doi.org/10.1001/archinte.159.22.2647.

Hofmann, A. F. 2009. The enterohepatic circulation of bile acids in mammals: Form and functions. Front. Biosci. (Landmark Ed.) 14:2584–2598. https://doi.org/10.2741/3399.

Honig, S. M., S. Fu, X. Mao, A. Yopp, M. D. Gunn, G. J. Randolph, and J. S. Bromberg. 2003. FTY720 stimulates multidrug transporter- and cysteinyl leukotriene-dependent T cell chemotaxis to lymph nodes. J. Clin. Invest. 111:627–637. https://doi.org/10.1172/JCI200316200.

Jäntti, S. E., M. Kivilompolo, L. Ohrnberg, K. H. Pietiläinen, H. Nygren, M. Orešič, and T. Hyötyläinen. 2014. Quantitative profiling of bile acids in blood, adipose tissue, intestine, and gall bladder samples using ultra high performance liquid chromatography-tandem mass spectrometry. Anal. Bioanal. Chem. 406:7799–7815. https://doi.org/10.1007/s00216-014-8230-9.

JASP Team. 2019. JASP Ver. 0.17.1. Accessed Nov. 1, 2022. https://jasp-stats.org/.

Jenkins, G. J., and L. Hardie. 2008. An overview of bile-acid synthesis, chemistry and function. Chapter 1 in Bile Acids: Toxicology and Bioactivity. 4th ed. Royal Society of Chemistry, Cambridge, UK.

Joseph, S. B., B. A. Laffitte, P. H. Patel, M. A. Watson, K. E. Matsukuma, R. Walczak, J. L. Collins, T. F. Osborne, and P. Tontonoz. 2002. Direct and indirect mechanisms for regulation of fatty acid synthase gene expression by liver X receptors. J. Biol. Chem. 277:11019–11025. https://doi.org/10.1074/jbc.M111041200.

Jung, D., B. Hagenbuch, M. Fried, P. J. Meier, and G. A. Kullak-Ublick. 2004. Role of liver-enriched transcription factors and nuclear recep-

tors in regulating the human, mouse, and rat NTCP gene. Am. J. Physiol. Gastrointest. Liver Physiol. 286:G752–G761. https://doi.org/10.1152/ajpgi.00456.2003.

Klaassen, C. D., and L. M. Aleksunes. 2010. Xenobiotic, bile acid, and cholesterol transporters: Function and regulation. Pharmacol. Rev. 62:1–96. https://doi.org/10.1124/pr.109.002014.

Kliewer, S. A., J. T. Moore, L. Wade, J. L. Staudinger, M. A. Watson, S. A. Jones, D. D. McKee, B. B. Oliver, T. M. Willson, R. H. Zetterström, T. Perlmann, and J. M. Lehmann. 1998. An orphan nuclear receptor activated by pregnanes defines a novel steroid signaling pathway. Cell 92:73–82. https://doi.org/10.1016/S0092-8674(00)80900-9.

LaRusso, N. F., N. E. Hoffman, M. G. Korman, A. F. Hofmann, and A. E. Cowen. 1978. Determinants of fasting and postprandial serum bile acid levels in healthy man. Am. J. Dig. Dis. 23:385–391. https://doi.org/10.1007/BF01072919.

Li, J., E. Daly, E. Campioli, M. Wabitsch, and V. Papadopoulos. 2014. De novo synthesis of steroids and oxysterols in adipocytes. J. Biol. Chem. 289:747–764. https://doi.org/10.1074/jbc.M113.534172.

Li, J., and P. A. Dawson. 2019. Animal models to study bile acid metabolism. Biochim. Biophys. Acta Mol. Basis Dis. 1865:895–911. https://doi.org/10.1016/j.bbadis.2018.05.011.

Lu, T. T., M. Makishima, J. J. Repa, K. Schoonjans, T. A. Kerr, J. Auwerx, and D. J. Mangelsdorf. 2000. Molecular basis for feedback regulation of bile acid synthesis by nuclear receptors. Mol. Cell 6:507–515. https://doi.org/10.1016/S1097-2765(00)00050-2.

Ma, H., and M. E. Patti. 2014. Bile acids, obesity, and the metabolic syndrome. Best Pract. Res. Clin. Gastroenterol. 28:573–583. https://doi.org/10.1016/j.bpg.2014.07.004.

Maruyama, T., Y. Miyamoto, T. Nakamura, Y. Tamai, H. Okada, E. Sugiyama, T. Nakamura, H. Itadani, and K. Tanaka. 2002. Identification of membrane-type receptor for bile acids (M-BAR). Biochem. Biophys. Res. Commun. 298:714–719. https://doi.org/10.1016/S0006-291X(02)02550-0.

Maruyama, T., K. Tanaka, J. Suzuki, H. Miyoshi, N. Harada, T. Nakamura, Y. Miyamoto, A. Kanatani, and Y. Tamai. 2006. Targeted disruption of G protein-coupled bile acid receptor 1 (Gpbar1/M-Bar) in mice. J. Endocrinol. 191:197–205. https://doi.org/10.1677/joe.1.06546.

Mast, N., R. Norcross, U. Andersson, M. Shou, K. Nakayama, I. Bjorkhem, and I. A. Pikuleva. 2003. Broad substrate specificity of human cytochrome P450 46A1 which initiates cholesterol degradation in the brain. Biochemistry 42:14284–14292. https://doi.org/10.1021/bi035512f.

McCreight, L. J., T. B. Stage, P. Connelly, M. Lonergan, F. Nielsen, C. Prehn, J. Adamski, K. Brøsen, and E. R. Pearson. 2018. Pharmacokinetics of metformin in patients with gastrointestinal intolerance. Diabetes Obes. Metab. 20:1593–1601. https://doi.org/10.1111/dom.13264.

Monte, M. J., J. J. G. Marin, A. Antelo, and J. Vazquez-Tato. 2009. Bile acids: Chemistry, physiology, and pathophysiology. World J. Gastroenterol. 15:804–816. https://doi.org/10.3748/wjg.15.804.

Pandak, W. M., and G. Kakiyama. 2019. The acidic pathway of bile acid synthesis: Not just an alternative pathway. Liver Res. 3:88–98. https://doi.org/10.1016/j.livres.2019.05.001.

Pham, H. T., K. Arnhard, Y. J. Asad, L. Deng, T. K. Felder, L. St John-Williams, V. Kaever, M. Leadley, N. Mitro, S. Muccio, C. Prehn, M. Rauh, U. Rolle-Kampczyk, J. W. Thompson, O. Uhl, M. Ulaszewska, M. Vogeser, D. S. Wishart, and T. Koal. 2016. Inter-laboratory robustness of next-generation bile acid study in mice and humans: International ring trial involving 12 laboratories. J. Appl. Lab. Med. 1:129–142. https://doi.org/10.1373/jalm.2016.020537.

Prawitt, J., and B. Staels. 2010. Bile acid sequestrants: glucose-lowering mechanisms. Metab. Syndr. Relat. Disord. 8(Suppl. 1):S3–S8. https://doi.org/10.1089/met.2010.0096.

Prinz, P., T. Hofmann, A. Ahnis, U. Elbelt, M. Goebel-Stengel, B. F. Klapp, M. Rose, and A. Stengel. 2015. Plasma bile acids show a positive correlation with body mass index and are negatively associated with cognitive restraint of eating in obese patients. Front. Neurosci. 9:199. https://doi.org/10.3389/fnins.2015.00199.

Rehage, J., K. Qualmann, C. Meier, N. Stockhofe-Zurwieden, M. Hoeltershinken, and J. Pohlenz. 1999. Total serum bile acid concentrations in dairy cows with fatty liver and liver failure. Dtsch. Tierarztl. Wochenschr. 106:26–29.

Reiter, S., A. Dunkel, C. Dawid, and T. Hofmann. 2021. Targeted LC-MS/MS profiling of bile acids in various animal tissues. J. Agric. Food Chem. 69:10572–10580. https://doi.org/10.1021/acs.jafc.1c03433.

Russell, D. W. 2000. Oxysterol biosynthetic enzymes. Biochim. Biophys. Acta Mol. Cell Biol. Lipids 1529:126–135. https://doi.org/10.1016/S1388-1981(00)00142-6.

Russell, D. W. 2003. The enzymes, regulation, and genetics of bile acid synthesis. Annu. Rev. Biochem. 72:137–174. https://doi.org/10.1146/annurev.biochem.72.121801.161712.

Saremi, B., H. Sauerwein, S. Dänicke, and M. Mielenz. 2012. Technical note: Identification of reference genes for gene expression studies in different bovine tissues focusing on different fat depots. J. Dairy Sci. 95:3131–3138. https://doi.org/10.3168/jds.2011-4803.

Schmid, A., J. Schlegel, M. Thomalla, T. Karrasch, and A. Schäffler. 2019. Evidence of functional bile acid signaling pathways in adipocytes. Mol. Cell. Endocrinol. 483:1–10. https://doi.org/10.1016/j.mce.2018.12.006.

Schuh, K., S. Häussler, H. Sadri, C. Prehn, J. Lintelmann, J. Adamski, C. Koch, D. Frieten, M. H. Ghaffari, G. Dusel, and H. Sauerwein. 2022. Blood and adipose tissue steroid metabolomics and mRNA expression of steroidogenic enzymes in periparturient dairy cows differing in body condition. Sci. Rep. 12:2297. https://doi.org/10.1038/s41598-022-06014-z.

Schuh, K., H. Sadri, S. Häussler, L. A. Webb, C. Urh, M. Wagner, C. Koch, J. Frahm, S. Dänicke, G. Dusel, and H. Sauerwein. 2019. Comparison of performance and metabolism from late pregnancy to early lactation in dairy cows with elevated v. normal body condition at dry-off. Animal 13:1478–1488. https://doi.org/10.1017/S1751731118003385.

Shapiro, H., A. A. Kolodziejczyk, D. Halstuch, and E. Elinav. 2018. Bile acids in glucose metabolism in health and disease. J. Exp. Med. 215:383–396. https://doi.org/10.1084/jem.20171965.

Sheriha, G. M., G. R. Waller, T. Chan, and A. D. Tillman. 1968. Composition of bile acids in ruminants. Lipids 3:72–78. https://doi.org/10.1007/BF02530972.

Studer, E., X. Zhou, R. Zhao, Y. Wang, K. Takabe, M. Nagahashi, W. M. Pandak, P. Dent, S. Spiegel, R. Shi, W. Xu, X. Liu, P. Bohdan, L. Zhang, H. Zhou, and P. B. Hylemon. 2012. Conjugated bile acids activate the sphingosine-1-phosphate receptor 2 in primary rodent hepatocytes. Hepatology 55:267–276. https://doi.org/10.1002/hep.24681.

Swann, J. R., E. J. Want, F. M. Geier, K. Spagou, I. D. Wilson, J. E. Sidaway, J. K. Nicholson, and E. Holmes. 2011. Systemic gut microbial modulation of bile acid metabolism in host tissue compartments. Proc. Natl. Acad. Sci. USA 108(Suppl. 1):4523–4530. https://doi.org/10.1073/pnas.1006734107.

Talukdar, S., and F. B. Hillgartner. 2006. The mechanism mediating the activation of acetyl-coenzyme A carboxylase-alpha gene transcription by the liver X receptor agonist T0–901317. J. Lipid Res. 47:2451–2461. https://doi.org/10.1194/jlr.M600276-JLR200.

Ticho, A. L., P. Malhotra, P. K. Dudeja, R. K. Gill, and W. A. Alrefai. 2019. Bile acid receptors and gastrointestinal functions. Liver Res. 3:31–39. https://doi.org/10.1016/j.livres.2019.01.001.

Timsit, Y. E., and M. Negishi. 2007. CAR and PXR: The xenobiotic-sensing receptors. Steroids 72:231–246. https://doi.org/10.1016/j.steroids.2006.12.006.

Trauner, M., and J. L. Boyer. 2003. Bile salt transporters: Molecular characterization, function, and regulation. Physiol. Rev. 83:633–671. https://doi.org/10.1152/physrev.00027.2002.

Velazquez-Villegas, L. A., A. Perino, V. Lemos, M. Zietak, M. Nomura, T. W. H. Pols, and K. Schoonjans. 2018. TGR5 signalling promotes mitochondrial fission and beige remodelling of white adipose tissue. Nat. Commun. 9:245. https://doi.org/10.1038/s41467-017-02068-0.

Wan, Y.-J. Y., and L. Sheng. 2018. Regulation of bile acid receptor activity. Liver Res. 2:180–185. https://doi.org/10.1016/j.livres.2018.09.008.

Washizu, T., I. Tomoda, and J. Kaneko. 1991. Serum bile acids composition of the dog, cow, horse and human. J. Vet. Med. Sci. 53:81–86. https://doi.org/10.1292/jvms.53.81.

Watanabe, M., S. M. Houten, C. Mataki, M. A. Christoffolete, B. W. Kim, H. Sato, N. Messaddeq, J. W. Harney, O. Ezaki, T. Kodama, K. Schoonjans, A. C. Bianco, and J. Auwerx. 2006. Bile acids induce energy expenditure by promoting intracellular thyroid hormone activation. Nature 439:484–489. https://doi.org/10.1038/nature04330.

West, H. J. 1990. Effect on liver function of acetonaemia and the fat cow syndrome in cattle. Res. Vet. Sci. 48:221–227. https://doi.org/10.1016/S0034-5288(18)30994-9.

Xie, C., W. Huang, R. L. Young, K. L. Jones, M. Horowitz, C. K. Rayner, and T. Wu. 2021. Role of bile acids in the regulation of food intake, and their dysregulation in metabolic disease. Nutrients 13:1104. https://doi.org/10.3390/nu13041104.

Yang, C. J., L. S. Wu, C. M. Tseng, M. J. Chao, P. C. Chen, and J. H. Lin. 2003. Urinary estrone sulfate for monitoring pregnancy of dairy cows. Asian-Australas. J. Anim. Sci. 16:1254–1260. https://doi.org/10.5713/ajas.2003.1254.

Zachut, M., and U. Moallem. 2017. Consistent magnitude of postpartum body weight loss within cows across lactations and the relation to reproductive performance. J. Dairy Sci. 100:3143–3154. https://doi.org/10.3168/jds.2016-11750.

ORCIDS

Lena Dicks https://orcid.org/0009-0007-5898-9949
Katharina Schuh-von Graevenitz https://orcid.org/0000-0003-0872-6394
Cornelia Prehn https://orcid.org/0000-0002-1274-4715
Hassan Sadri https://orcid.org/0000-0003-1802-4169
Eduard Murani https://orcid.org/0000-0002-3939-6255
Morteza Hosseini Ghaffari https://orcid.org/0000-0002-5811-3492
Susanne Häussler https://orcid.org/0000-0002-5197-541X